

1 Title: **Shared Song Object Detector Neurons in *Drosophila* Male and Female Brains**

2 **Drive Divergent, Sex-Specific Behaviors**

3

4 Authors: Jan Clemens<sup>1,2\*</sup>, David Deutsch<sup>1\*</sup>, Stephan Y. Thiberge<sup>1,3</sup>, and Mala Murthy<sup>1,3,4,#</sup>

5 Affiliations:

6 <sup>1</sup> Princeton Neuroscience Institute, Princeton University, Princeton 08540, NJ, USA

7 <sup>2</sup> current address: European Neuroscience Institute, Grisebachstrasse 5, Göttingen,

8 Germany

9 <sup>3</sup> Bezos Center for Neural Circuit Dynamics, Princeton Neuroscience Institute, Princeton  
10 University, Princeton, NJ, USA

11 <sup>4</sup> Department of Molecular Biology, Princeton University, Princeton, NJ, USA

12 \* These authors contributed equally

13 # Lead contact

14

15 Correspondence: mmurthy@princeton.edu

16 Running Title: Shared Song Detector Neurons Drive Sex-Specific Behaviors

17

18

19   **Abstract:**

20   Males and females often produce distinct responses to the same sensory stimuli. How such  
21   differences arise – at the level of sensory processing or in the circuits that generate behavior  
22   – remains largely unresolved across sensory modalities. We address this issue in the  
23   acoustic communication system of *Drosophila*. During courtship, males generate time-  
24   varying songs, and each sex responds with specific behaviors. We characterize male and  
25   female behavioral tuning for all aspects of song, and show that feature tuning is similar  
26   between sexes, suggesting sex-shared song detectors drive divergent behaviors. We then  
27   identify higher-order neurons in the *Drosophila* brain, called pC2, that are tuned for multiple  
28   temporal aspects of one mode of the male's song, drive sex-specific behaviors, and show a  
29   mirrored correspondence between sensory and motor tuning. We thus uncover acoustic  
30   object detector neurons at the sensory-motor interface that flexibly link auditory perception  
31   with sex-specific behavioral responses to communication signals.

32

33 **Introduction**

34 Across animals, males and females produce distinct, dimorphic behaviors in response to  
35 common sensory stimuli (e.g., pheromones, visual cues, or acoustic signals), and these  
36 differences are critical for social and reproductive behaviors (Billeter and Levine, 2013;  
37 Dulac and Wagner, 2006; Kelley, 2003; Yamamoto et al., 2013; Yang and Shah, 2014). The  
38 molecular dissection of sexual dimorphisms in the nervous system of flies and mice in  
39 particular (Cachero et al., 2010; Dulac and Wagner, 2006; Rideout et al., 2010; Stowers and  
40 Logan, 2010; Yang and Shah, 2014; Yu et al., 2010) has identified neurons involved in either  
41 processing important social cues or driving social behaviors, but it remains open as to how  
42 sex-specific behaviors to common sensory signals emerge along sensorimotor pathways. It  
43 could be that males and females process sensory information differently, leading to different  
44 behavioral outcomes, or that males and females process sensory information identically, but  
45 drive different behaviors downstream of common detectors.

46

47 This issue has been most heavily investigated for pheromone processing, and these studies  
48 point to differences along sensory pathways. For instance, in *Drosophila*, the male  
49 pheromone cVA induces either aggression in males (Wang and Anderson, 2010) or  
50 receptivity in females (Billeter et al., 2009; Kurtovic et al., 2007). The pheromone is detected  
51 by shared circuits in males and females and the similarly processed sensory information  
52 (Datta et al., 2008) is then routed to sex-specific higher-order olfactory neurons (Kohl et al.,  
53 2013; Ruta et al., 2010) that likely exert different effects on behavior, although this  
54 hypothesis has not yet been tested. In the mouse, the male pheromone ESP1 triggers  
55 lordosis in females, but has no effect on male behavior. This pheromone activates V2Rp5  
56 sensory neurons in both sexes but, analogous to cVA processing in flies, these neurons  
57 exhibit sex-specific projection patterns in the hypothalamus that drive sex-specific behavioral  
58 responses (Haga et al., 2010; Ishii et al., 2017). For pheromone processing then, the rule  
59 appears to be that early olfactory processing is largely shared between the sexes and then  
60 common percepts are routed to separate higher-order neurons or circuits for control of  
61 differential behaviors. But does this rule apply for other modalities, or for stimuli that can be  
62 defined by multiple temporal or spatial scales (e.g. visual objects or complex sounds). For  
63 such stimuli, selectivity typically emerges in higher-order neurons (Dicarlo et al., 2012;  
64 Gentner, 2008; Tsao and Livingstone, 2008) and we do not yet know if such neurons are  
65 shared between males and females, and therefore if dimorphic responses emerge in  
66 downstream circuits.

67

68 Here, we investigate this issue in the auditory system in *Drosophila*. Similar to birds (Fortune  
69 et al., 2011; Konishi, 1985), frogs (Gerhardt and Huber, 2002), or other insects (Ronacher et  
70 al., 2014), acoustic communication in *Drosophila* involves different behaviors in males and  
71 females relative to the courtship song. During courtship, males chase females and produce  
72 a species-specific song that comprises two major modes – pulse song consists of trains of  
73 brief pulses and sine song consists of a sustained harmonic oscillation (Bennet-Clark and  
74 Ewing, 1967). In contrast with males, females are silent but arbitrate mating decisions  
75 (Bennet-Clark and Ewing, 1969). Males use visual feedback cues from the female (rapid  
76 changes in her walking speed and her distance relative to him) to determine which song  
77 mode (sine or pulse) to produce over time (Clemens et al., 2017; Coen et al., 2014; 2016) –  
78 this gives rise to the variable structure of song bouts (Fig. 1A). Receptive females slow in  
79 response to song (Aranha et al., 2017; Bussell et al., 2014; Clemens et al., 2015; Coen et  
80 al., 2014; Cook, 1973; Crossley et al., 1995; F. Von Schilcher, 1976; Tompkins et al., 1982),  
81 while playback of courtship song to males can induce them to increase their walking speed  
82 (Crossley et al., 1995; F. Von Schilcher, 1976; Vaughan et al., 2014), and to display  
83 courtship-like behaviors (Eberl et al., 1997; Li et al., 2018; Yoon et al., 2013; Zhou et al.,  
84 2015). These behavioral differences surrounding song production and perception between  
85 *Drosophila* males and females, combined with the wealth of genetic and neural circuit tools,  
86 make the *Drosophila* acoustic communication system an excellent one in which to  
87 investigate whether males and females share common sensory detection strategies for their  
88 courtship song, and how divergent behaviors arise.

89

90 Each major mode of *Drosophila* courtship song, sine or pulse, contains patterns on multiple  
91 temporal scales (Arthur et al., 2013; Bennet-Clark and Ewing, 1967) (Fig. 1A) – neurons that  
92 represent either the pulse or sine mode should in theory bind all of the temporal features of  
93 each mode, similar to object detectors in other systems (Bizley and Cohen, 2013; Dicarlo et  
94 al., 2012; Gentner and Margoliash, 2003; Griffiths and Warren, 2004), and their tuning  
95 should match behavioral tuning. Historically, behaviorally relevant song features have been  
96 defined based on the parameters of the species' own song (Bennet-Clark and Ewing, 1969).  
97 However, there is now ample evidence that the preferred song can diverge from the  
98 conspecific song (Amézquita et al., 2011; Blankers et al., 2015; Ryan et al., 2001) – for  
99 instance if females prefer exaggerated song features (Rosenthal and Ryan, 2011; Ryan and  
100 Cummings, 2013) or respond to signal parameters not normally produced by their male

101 conspecifics (Hennig et al., 2016). Moreover, the job of the female nervous system is not  
102 only to tell one species apart from another, but also to select a particular mate from within  
103 the species distribution. It is therefore important to define song modes by the acoustic tuning  
104 of specific behavioral outputs. This has been done for other insects (e.g. (Clemens and  
105 Hennig, 2013; D. von Helversen and O. von Helversen, 1997)) but never for flies in a  
106 systematic way that also permits a direct comparison between sexes.  
107

108 To that end, we developed a behavioral assay for assessing dynamic changes in walking  
109 speed in response to sound playback in both sexes, and we then measured locomotor  
110 tuning for all features of either pulse or sine song. This reveals that males and females have  
111 similar tuning but different behavioral responses and that they are tuned for every major  
112 feature of the song. We then identified a small set of sexually dimorphic neurons, termed  
113 pC2 (Kimura et al., 2015; Rideout et al., 2010; Zhou et al., 2014), that serve as shared  
114 pulse song detectors in both sexes: the tuning of pC2 neurons is matched to behavioral  
115 tuning for pulse song – but not for sine song – across a wide range of temporal scales. We  
116 find that optogenetic activation of pC2 is sufficient to drive sex-specific behaviors produced  
117 in response to pulse song – changes in locomotion with sex-specific dynamics as well as  
118 singing in males. pC2 is also part of a sensorimotor loop, since it drives and is driven by  
119 pulse song. Finally, we establish the importance of pC2 neurons by showing that early social  
120 experience changes both the tuning of these neurons and the tuning of the behavior. Our  
121 results indicate that the fly brain contains common song object detectors in males and  
122 females which control sex-specific behavioral responses to song via downstream circuits.  
123

124 **Results**

125 **Comprehensive characterization of behavioral tuning for courtship song features**

126 We designed a single-fly playback assay in which individual males or females receive  
127 acoustic stimuli in the absence of any confounding social interactions, and we implemented  
128 an automated tracker to analyze changes in locomotion relative to acoustic playback (Fig.  
129 1B and Movie S1). The assay (which we refer to as FLyTRAP (**Fly Locomotor TRacking and**  
130 **Acoustic Playback**)) monitors dynamic changes in walking speed, which provides a readout  
131 that can be directly compared between both males and females, as opposed to slower  
132 readouts of sex-specific behaviors such as the female time to copulation (Bennet-Clark and  
133 Ewing, 1969; Zhou et al., 2014) or male-male chaining (Yoon et al., 2013; Zhou et al., 2015).  
134 Because of the high-throughput nature of our assay combined with automated tracking, we

135 can easily test a large number of flies and song parameters, including those only rarely  
136 produced by conspecifics but to which animals might be sensitive (Coen et al. 2014; Aranha  
137 et al., 2017; Bussell et al., 2014; Crossley et al., 1995; Eberl et al., 1997; Rybak et al.,  
138 2002a; 2002b; F. Von Schilcher, 1976; Yoon et al., 2013; Zhou et al., 2015).

139

140 Previous studies that assayed either male-female copulation rates or male-male chaining  
141 often focused on behavioral selectivity for the interval between pulses in a pulse train (inter-  
142 pulse interval (IPI), Fig. 1A) (Bennet-Clark and Ewing, 1969; Rybak et al., 2002b; F. Von  
143 Schilcher, 1976; Zhou et al., 2015). Using FLyTRAP, we systematically compared male and  
144 female locomotor tuning to 82 acoustic stimuli that span the features and timescales present  
145 in courtship song (see Supplemental Table 1). Typically, each stimulus was presented 23  
146 times to 120 females and 120 males, generating >2500 responses per stimulus and sex (see  
147 Methods).

148

149 We started by examining behavioral tuning for IPI using the wild type strain NM91. We  
150 generated artificial pulse trains and varied only the IPI (between 16 and 96ms) – we chose a  
151 stimulus intensity of 5 mm/s since varying intensity had minimal effect on pulse song  
152 responses in females (Fig. S1A, B). Observed changes in speed were stimulus-locked, sex-  
153 specific and tuned to IPI (Fig. 1C). While females slow down to pulse trains, males exhibit  
154 transient slowing at pulse train onset followed by a long-lasting acceleration. The transient  
155 component of the locomotor response was present for all stimuli (Fig. S1C, D, S2A-C) and  
156 may correspond to an unspecific startle response to sound onset (Lehnert et al., 2013). The  
157 transient was also present in females but masked by the stimulus-dependent slowing that  
158 followed (Fig. 1C). Due to the briefness of the transient response, the integral change in  
159 speed following stimulus onset reflects mostly the speed during the sustained phase (Fig.  
160 S1C, D). For simplicity, we therefore used the full integral as an overall measure of  
161 behavioral tuning. We found that in FLyTRAP, female IPI tuning is a band-pass filter  
162 matched to the statistics of male song (Fig. 1D): the mode of the distribution of *Drosophila*  
163 *melanogaster* IPIs is centered between 30 and 50 ms and females decrease their speed  
164 most for the same IPI range, and less for shorter or longer IPIs. Males produced a similar  
165 band-pass tuning curve peaked at the same IPI range - but their locomotor response was  
166 opposite in sign (males accelerated, females decelerated). This is consistent with the results  
167 of other assays that have found band-pass tuning for IPI in both sexes (Bennet-Clark and

168 Ewing, 1969; Rybak et al., 2002b; F. Von Schilcher, 1976; Zhou et al., 2015) and a sex-  
169 specific sign of locomotor responses (Crossley et al., 1995; F. Von Schilcher, 1976).

170

171 We next systematically varied parameters that characterize pulse song to cover (and extend  
172 beyond) the distribution of each parameter within *D. melanogaster* male song (just as we did  
173 for IPI) (see Supp. Fig. 2). We examined behavioral tuning in both sexes for parameters that  
174 varied on timescales of milliseconds (carrier frequency, pulse duration and IPI) to seconds  
175 (pulse train duration) (Fig. 1A). We found that male and female tuning curves are of opposite  
176 sign but similar shape for all pulse song features tested across time scales (Fig. 2A, B, S2D-  
177 F, see Fig. S2A-C for speed traces), and that the behavioral tuning for pulse parameters  
178 often overlapped the distribution found in natural song (Fig. 2C). While the behavioral tuning  
179 curves for all pulse song features on short time scales are band-pass with a well-defined  
180 peak, we found that tuning for pulse train duration was monotonous: both females and males  
181 increase their locomotor response with increasing pulse train duration up to four seconds  
182 (Fig. 2A, B). During natural courtship, pulse trains longer than four seconds are rarely  
183 produced (Coen et al., 2014). Males also produce two distinct types of pulses (Clemens et  
184 al., 2017) – we find that while females appear to be broadly tuned for both types of pulses in  
185 the FLyTRAP assay, males respond preferentially to higher frequency pulses. Finally, we  
186 found that both males and females are more selective for the pulse duration versus the  
187 pulse pause, the two components of the IPI (Fig. S2D-F) – this is in contrast to other insects  
188 that produce and process song pulses (e.g. crickets, grasshoppers, katydids), and that are  
189 preferentially tuned to pulse pause, pulse period or pulse train duty cycle (Hennig et al.,  
190 2014; Ronacher et al., 2014).

191

192 We next tested locomotor tuning for the parameters that characterize sine stimuli – carrier  
193 frequency and the duration of sine trains (Fig. 1A). Both males and females slow for sine  
194 tones of different frequencies, with very low and very high frequencies eliciting the strongest  
195 responses (Fig. 2A, B and Fig. S2A-C). Notably, the frequencies inducing the strongest  
196 slowing (100Hz) are not typically produced by males (Fig. 2C). As for sine train duration  
197 tuning, we observed sustained responses that increased with duration and saturated only  
198 weakly, possibly because of the weak response magnitude.

199

200 Pulse and sine song usually co-occur within a single bout but it is not known why males  
201 produce two different modes (although females respond to both during natural courtship

202 (Clemens et al., 2017; Coen et al., 2014)). One possibility is that one mode exerts a priming  
203 effect on the other (F. V. Schilcher, 1976). To test interactions between the two song modes,  
204 we presented sequences in which a 2-second pulse train was followed by a 2-second sine  
205 tone or in which a sine tone was followed by a pulse train and compared the responses for  
206 these sequences to the responses to an individual pulse train or sine tone (Fig. S2G). The  
207 responses are well explained by a linear combination of the responses to individual sine or  
208 pulse trains. Deviations from linearity occur due to sound onset responses, but otherwise  
209 responses do not strongly depend on the order of presentation in a bout (see also (Talyn  
210 and Dowse, 2004)). This suggests that these stimuli are processed in independent  
211 pathways.

212

213 To summarize, we compared behavioral responses in males and females for all features that  
214 define the courtship song. We found that male and female speed changes were strongly  
215 correlated for both song modes but that the sign of the correlation was negative for pulse  
216 stimuli and positive for sine stimuli (Fig. 2E). The opposite sign of the correlations along with  
217 the independence of responses to sine and pulse stimuli (Fig. S2G) indicates that sine and  
218 pulse song are processed by different circuits. The large magnitude of the correlations  
219 implies that feature tuning of the behavioral responses is similar between sexes and  
220 suggests that detector neurons for each song mode should be shared between sexes.

221

## 222 **Hearing pulse song drives wing extension in males, but not in females**

223 Another sex-specific aspect of song responses is courtship: playback of conspecific song  
224 induces courtship-like behavior in males – this can even be directed towards other males,  
225 leading to the male chaining response, in which males follow other males, chasing and  
226 extending their wings (Eberl et al., 1997; F. Von Schilcher, 1976; Yoon et al., 2013). In our  
227 single-fly assay, males lack a target for courtship and the song-induced arousal likely  
228 manifests as an increase in speed. Since FLyTRAP does not permit simultaneous recording  
229 of fly acoustic signals during playback, we quantified wing extension as a proxy for singing,  
230 and examined whether song playback alone drives singing in solitary males. We found that  
231 solitary males extend their wings in response to pulse song stimuli specifically (Fig. 2F, G,  
232 Movie S2). This behavior is tuned for the inter-pulse interval (similar to the locomotor  
233 response, Fig. 1D) – the conspecific IPI of 36ms drives the most wing extension, and shorter  
234 and longer IPIs evoke fewer wing extensions. By contrast, conspecific sine song (150Hz)  
235 does not induce wing extension (Fig. 2F) (see also (Eberl et al., 1997; Yoon et al., 2013)).

236 We also found that playback of pulse does not elicit wing extension in females, even though  
237 females have been shown to possess functional circuitry for singing (Clyne and Miesenböck,  
238 2008; Rezával et al., 2016) – wing extension in response to pulse song is thus sex-specific.  
239

240 These results are consistent with those for locomotor tuning: pulse song, but not sine song,  
241 generates sex-specific differences in behavior. The identical tuning of the two behavioral  
242 responses in males (locomotion (Fig. 1C) and song production (Fig. 2G)) suggests that the  
243 behavioral responses are driven by a common circuit. Finally, that playback of pulse song  
244 alone is sufficient to drive singing in males implies the existence of neurons with  
245 sensorimotor correspondences, similar to “mirror neurons” (Mooney, 2014; Prather et al.,  
246 2008; Rizzolatti and Arbib, 1998) – we explore this hypothesis below.  
247

#### 248 ***Drosophila* male and female brains share pulse song detector neurons**

249 Our systematic exploration of song stimulus space using the FLyTRAP assay revealed  
250 behavioral tuning for song parameters across temporal scales (from the carrier frequencies  
251 of sine and pulse lasting milliseconds to the duration of sine and pulse trains lasting  
252 seconds). We next searched for neurons with tuning across temporal scales that could serve  
253 as object detectors of either the pulse or sine mode of courtship song. We focused on  
254 neurons expressing the Doublesex (Dsx) transcription factor that regulates sexual  
255 dimorphism in cell number and neuronal morphology between males and females. In the  
256 central brain there are ~70 Dsx+ neurons per hemisphere in females and ~140 Dsx+  
257 neurons per hemisphere in males (Kimura et al., 2015; Rideout et al., 2010). Previous  
258 studies found calcium responses to both song-like stimuli and pheromones in Dsx+ neuron  
259 projections in females (Zhou et al., 2014) and tuning for the inter-pulse interval in males  
260 (Zhou et al., 2015). In addition, silencing subsets of Dsx+ neurons in females affected  
261 receptivity (Zhou et al., 2014). These data suggest that Dsx+ neurons could serve as the  
262 common pulse song detectors in males and females. To test this possibility, we recorded  
263 auditory responses in Dsx+ neurons and examined tuning for song features across  
264 timescales, in both males and females, to compare with our behavioral results.  
265

266 We imaged neural activity using the calcium sensor GCaMP6m (Chen et al., 2013)  
267 expressed only in Dsx+ neurons and focused on the lateral junction (LJ) (Cachero et al.,  
268 2010; Ito et al., 2014; Yu et al., 2010), a site of convergence for the majority of Dsx+ neuron  
269 projections (Fig. 3A, B, S5B, C, Movie S3, S4). We found that male and female Dsx+

270 projections in the LJ are driven strongly by pulse, but not by sine, stimuli (Fig. 3C) similar to  
271 previous results (Zhou et al., 2014). While males overall produce weaker responses to  
272 auditory stimuli compared with females (Fig. 3C), the normalized LJ responses are highly  
273 correlated between sexes – stimuli that evoked the strongest responses in females also  
274 evoked the strongest responses in males (Fig. 3D).

275

276 In order to connect behavioral tuning to neural tuning, we validated that the genetic strain in  
277 which we imaged calcium responses possessed the same behavioral tuning as the strain  
278 used in FLyTRAP (Fig. S3A). The sex-specific sign and shape of the IPI tuning curves of  
279 flies from these two strains matches acoustic tuning measured in other playback assays:  
280 females slow for pulse song (Clemens et al., 2017; Coen et al., 2014; Crossley et al., 1995;  
281 F. Von Schilcher, 1976) and copulate most when exposed to conspecific IPIs and less for  
282 shorter or longer IPIs (Bennet-Clark and Ewing, 1969; Li et al., 2018); males in groups  
283 increase their speed (Crossley et al., 1995; F. Von Schilcher, 1976; Vaughan et al., 2014)  
284 and court other females or males most when exposed to pulse song with the conspecific IPI  
285 (Crossley et al., 1995; Yoon et al., 2013; Zhou et al., 2015). The two strains chosen for the  
286 behavioral and calcium imaging experiments thus display the species-typical acoustic tuning  
287 likely expressed during natural courtship encounters. Interestingly, the behavioral tuning for  
288 IPI in seven additional wild type strains is still sex-specific but deviates from the species-  
289 typical tuning (Fig. S3B) when assayed in FLyTRAP, even though the same wild type strains  
290 – including NM91 – display virtually identical responses to song in a courtship assay in  
291 which a male courts a female (Clemens et al., 2017; 2015; Coen et al., 2016; 2014). This  
292 indicates that these strains require additional cues (e.g., pheromones or visual cues) to fully  
293 express their preference for conspecific song features.

294

295 When examining neuronal tuning curves, we found a good match between Dsx+ LJ  
296 responses and the magnitude of changes in speed across all timescales of pulse song in  
297 both sexes (Fig. 3E, F). For example, the Dsx+ LJ tuning curve for IPI is similar in females  
298 and males with the strongest responses at 36ms, matching the behavioral tuning curves  
299 (compare with Fig. 2A,B) – moreover, Dsx+ neurons are also preferentially tuned for the  
300 pulse duration over the pulse pause (Fig. S4D, E – compare with Fig. S2E, F). At longer  
301 timescales, LJ tuning curves also match behavioral tuning curves for pulse train duration –  
302 while the integral calcium continues to increase with train duration, the peak fluorescence  
303 saturates in both sexes, similar to the behavioral response. Apart from this difference, peak

304 and integral  $\Delta F/F$  are similar (Fig. S4F, G). Overall, LJ responses are selective for the  
305 features found in conspecific pulse song: LJ responses were strongest for stimuli with a  
306 carrier frequency of 250Hz, an inter-pulse interval of 36ms, and a pulse duration of 16ms  
307 (Fig. S4A-C). A match in only two of these three features was not sufficient to maximally  
308 drive Dsx+ neurons. Sine stimuli have lower carrier frequencies, long durations, and no  
309 pauses (they are by definition continuous) – which explains the weak responses of Dsx+  
310 neurons to all sine stimuli (Fig. 3C).

311

312 We next directly compared Dsx+ LJ responses and behavioral responses for all stimuli and  
313 found strong correlations for pulse stimuli in both sexes – although with a sex-specific sign.  
314 That is, male neural and behavioral tuning for pulse stimuli are positively correlated ( $r=0.55$ ,  
315  $p=9\times 10^{-6}$ ) – high Dsx+ neuron activity correlates with the most acceleration (Fig. 3G).  
316 Female neural and behavioral tuning for pulse stimuli are negatively correlated ( $r=-0.62$ ,  
317  $p=2\times 10^{-7}$ ) – high Dsx+ neuron activity correlates with the most slowing (Fig. 3H). This is  
318 consistent with these neurons controlling the magnitude, but not the direction of speed  
319 changes. We observed no statistically significant correlation for sine stimuli (male:  $r=-0.15$ ,  
320  $p=0.56$ ; female:  $r=0.27$ ,  $p=0.30$ ), as Dsx+ LJ responses to sine stimuli were weak. Note that  
321 Dsx+ LJ activity only accounts for roughly 1/3 of the variability in behavioral responses for  
322 pulse song. This suggests that the behavior is driven and modulated by additional pathways  
323 outside of the Dsx+ neurons in the LJ. Nonetheless, Dsx+ neurons that innervate the LJ  
324 have tuning properties expected for pulse song object detectors – they prefer pulse over  
325 sine stimuli, are similarly tuned in males and females, and their feature tuning matches the  
326 behavioral tuning for all pulse, but not sine, stimuli across timescales.

327

### 328 **Dsx+ pC2I neurons are pulse song detectors**

329 The Dsx+ neurons of the central brain form a morphologically heterogeneous population with  
330 several distinct, anatomical clusters many of which project to the LJ (Kimura et al., 2015;  
331 Rideout et al., 2010; Zhou et al., 2015; 2014) (Fig. 3A). Previous studies that examined  
332 auditory responses in Dsx+ neurons (Zhou et al., 2015; 2014) did not resolve which subtype  
333 carried the response. Using a stochastic labeling approach (Nern et al., 2015), we confirmed  
334 that only five out of eight Dsx+ cell types in the female brain project to the LJ (Kimura et al.,  
335 2015): pC1, pC2I/m, pMN1, and pMN2, but not pCd1/2 and aDN (Fig. 4A and Fig. S5D, E).  
336 We next imaged calcium responses to pulse and sine stimuli in the somata of all five Dsx+  
337 cell types that innervate the LJ and found that a subset of neurons in the pC1 and pC2

338 clusters possess auditory responses, in addition to cell type pMN2 (a female-specific neuron  
339 (Kimura et al., 2015) comprising only one cell body per hemisphere) (Fig. 4B, C, Movie S5,  
340 S6). All responsive cells preferred pulse over sine stimuli (Fig. 4D). We did not observe  
341 auditory responses in pMN1 neurons (not shown), although we cannot rule out that this  
342 neuron class has responses that are below the level of detection by the calcium indicator  
343 GCaMP6m.

344

345 The pC1 cluster contained a small number of auditory cells (2-3 cells in the female brain; we  
346 found none in the male brain) (Fig. 4C). Since pC1 and pNM2 contain only few auditory-  
347 responsive neurons and/or are present only in females, we focused on pC2 as the putative  
348 pulse song detector common to both sexes. Although there are more pC2 neurons in males  
349 versus females (~67 vs. ~26, (Kimura et al., 2015)) the number of auditory ROIs is similar in  
350 both sexes (~15). pC2 neurons can be subdivided into a lateral and a medial type, termed  
351 pC2l and pC2m (Robinett et al., 2010), and each type projects to the lateral junction via a  
352 distinct process (see Fig. 3A, S5B, C). Most auditory ROIs were lateral in the pC2 cluster  
353 (Fig. S5A), and all somata as well as the pC2l process produced strong auditory responses  
354 that were highly correlated with those we recorded in the LJ (Fig. 4F, G). From this we  
355 conclude that LJ responses reflect the tuning of pC2l neurons. Importantly, the tuning of the  
356 pC2l process matches the behavioral tuning (Fig. 4H), indicating that pC2l neurons are pulse  
357 song object detectors.

358

### 359 **Optogenetic activation of pC2l neurons drives sex-specific behaviors**

360 If pC2l neurons serve as pulse song detectors, then their activation should also be sufficient  
361 to drive the sex-specific behaviors observed for pulse song – changes in locomotion and  
362 singing that are distinct between males and females. To test this hypothesis, we used a  
363 driver line (Zhou et al., 2014; Rezával et al., 2016) that labels 11/22 female and 22/36 male  
364 pC2l neurons, in addition to 5-6 pCd neurons, but no pC2m or pC1 neurons (Fig. S6A). At  
365 least 5 of the pC2l cells in this driver line responded to song (Fig. S6B), which corresponds  
366 to ~1/3 of the auditory pC2l neurons. We expressed CsChrimson, a red-shifted  
367 channelrhodopsin (Klapoetke et al., 2014), in these neurons and optogenetically activated  
368 them in both males and females.

369

370 We first recorded behavior in a chamber tiled with microphones (Coen et al., 2014) to test  
371 whether pC2 activation was sufficient to induce singing, as we previously showed that pulse

372 song playback alone drives wing extension in males (Fig. 2F, G). Upon red light activation,  
373 males produced pulse song, while sine song was produced transiently after stimulus offset  
374 (Fig. 5A, Movie S7), and the amount of pulse song produced scaled with the strength of  
375 activation (Fig. 5B). The evoked pulse and sine songs were virtually indistinguishable from  
376 natural song (Fig. S6C, D). In *Drosophila*, retinal (the channelrhodopsin cofactor) must be  
377 supplied via feeding, and red light stimulation drove singing significantly more in males fed  
378 with retinal versus those fed regular food (Fig. S6E). Activation of a control line that only  
379 labels pCd neurons (Zhou et al., 2014) did not drive any singing (Fig. S6E), implying that  
380 song production results from the activation of the pC2 neurons in our driver. Importantly, we  
381 never observed song production upon pC2 activation in females (Fig. S6E) – pC2 neurons  
382 thus drive song in a sex-specific manner. These results also establish pC2 neurons as  
383 serving a dual sensory and motor role, analogous to “mirror neurons” in other systems  
384 (Mooney, 2014): they respond selectively to the pulse song (Fig. 3C, F) and also bias the  
385 song pathway towards producing the same song mode (Fig. 5A, B).

386  
387 We next evaluated changes in locomotor speed in both sexes for multiple levels of  
388 optogenetic activation by placing flies in the FLyTRAP assay but using red light for activation  
389 (instead of sound). To account for innate visual responses to the light stimulus, we  
390 subtracted the responses of normally fed flies from retinal fed flies (Fig. S6F). Because the  
391 behavioral responses to acoustic stimuli can depend on genetic background (Fig. S3), we  
392 assessed responses to playback of pulse stimuli with varying IPI for the genotype used in  
393 the optogenetic activation experiments (see Methods for list of genotypes). For this particular  
394 strain, both males and females decreased their walking speed in response to pulse stimuli.  
395 Nonetheless, we observed sex-specific differences in both the magnitude and dynamics of  
396 the behavioral responses to sound (Fig. 5D-G), and optogenetic activation of pC2 neurons  
397 reproduced many of these sex-specific differences (Fig. 5 H-K). For instance, male  
398 responses outlasted the stimulus for both sound and optogenetic activation, while female  
399 responses were multiphasic for both conditions. To confirm that the response dynamics  
400 were sex-specific, we performed principal component analysis (PCA) on the speed traces of  
401 males and females for sound playback and optogenetic activation experiments (Fig. 5L). The  
402 first two principal components were sufficient to explain 84% of the variance in the speed  
403 traces, and the responses varied along sex-specific axes: the PCA scores for males varied  
404 most in the direction of the first principal component and female PCA scores align with the  
405 orthogonal, second principal component. In each sex, responses for acoustic and

406 optogenetic stimulation were co-aligned, suggesting that pC2 neuron activation recapitulates  
407 the sex-specific locomotor dynamics observed for acoustic playback in this strain.

408

409 Finally, we used the same pC2-specific driver to constitutively suppress the synaptic output  
410 of pC2 (via expression of TNT (Sweeney et al., 1995)) in females and paired them with wild  
411 type virgin males (see Methods). We quantified female song responses as the correlation  
412 between different song features and female speed (Clemens et al., 2015; Coen et al., 2014)  
413 (Fig. 5M-O). Because male song is structured via sensory feedback cues from the female  
414 (Coen et al., 2014), silencing pC2 neurons in females could affect the content of male song  
415 – however, the statistics of male song were unchanged by the female manipulation (Fig.  
416 S6G-H). pC2 inactivation specifically affected the correlation between female speed and the  
417 pulse song IPI, which changed from ~0 to 0.3 (Fig. 5M-O). While control – and wild type  
418 (Clemens et al., 2015) – females do not change their speed relative to the range of natural  
419 IPIs produced by conspecific males, females with pC2 neurons silenced accelerate more  
420 with increasing IPI. This indicates that pC2 neurons are required for the proper response to  
421 pulse song, and that other neurons that represent pulse song are tuned for longer IPIs.  
422 While female locomotor responses to courtship song were affected by pC2 inactivation,  
423 copulation rates were not significantly reduced (Fig. S6I), consistent with previous studies  
424 (Zhou et al., 2014). In conjunction with the match between behavioral tuning and pC2 tuning,  
425 these results add to the evidence that pC2 neurons serve as pulse song object detectors  
426 and play a critical role at the sensorimotor interface – they relay information about pulse  
427 song to sex-specific downstream circuits that control either singing or locomotion, and  
428 thereby mediate acoustic communication behaviors.

429

### 430 **pC2 neural activity is modulated by social experience**

431 Many sexual behaviors change with social experience (Keleman et al., 2012; Li et al., 2018;  
432 Marlin et al., 2015; Remedios et al., 2017). This plasticity could be mediated by modulating  
433 the selectivity and the gain of object detectors or that of downstream circuits. Social  
434 experience is known to affect courtship behavior in *Drosophila* (Ellis and Kessler, 1975;  
435 Kohatsu and Yamamoto, 2015; F. Von Schilcher, 1976), and prolonged exposure to  
436 conspecific song sharpens the IPI selectivity of the female mating decision and the male  
437 chaining response (Li et al., 2018). We first tested whether locomotor responses in  
438 FLyTRAP are also modulated by social experience. We found that males that were exposed  
439 to social cues (including the song of other males) via group-housing exhibited stronger and

440 more selective changes in speed than individually housed males (Fig. 6A). Females do not  
441 sing to other females when group housed and accordingly, their locomotor responses were  
442 unaffected by housing conditions (Fig. 6A). These sex-specific effects of housing were  
443 reflected in changes in the neuronal responses of pC2 neurons: calcium responses in pC2  
444 (measured via the LJ) (Fig. 4F,G) do not change strongly with housing conditions in females,  
445 but become more selective for IPI in group-housed males (Fig. 6B). Notably, sine song  
446 responses and responses to pulse trains with different durations are not affected by housing  
447 conditions (Fig. S7).

448

#### 449 **Discussion**

450 Using a quantitative behavioral assay, we characterized locomotor responses in both males  
451 and females to the features that define the *Drosophila melanogaster* courtship song. Males  
452 and females showed similar tuning for pulse song stimuli, but nonetheless produced distinct  
453 responses (for example, males accelerate while females decelerate; males sing while  
454 females do not) (Fig. 1, 2). Both males and females were responsive to all features of pulse  
455 song, across timescales, and tuning was matched to the distribution of each parameter in  
456 the male's song. We then identified Dsx+ pC2 neurons in the brain that respond selectively  
457 to pulse song stimuli, and whose tuning is matched to behavioral tuning (Fig. 3, 4). The  
458 activation of pC2 neurons elicited sex-specific behavioral responses to pulse song (Fig. 5),  
459 and social experience sharpened both behavioral feature selectivity and pC2 tuning (Fig. 6).  
460 We thus conclude that Dsx+ pC2 neurons are pulse song object detectors that couple song  
461 detection with the execution of sex-specific behaviors.

462

463 In other systems, object detectors are typically higher-order neurons that bind the multiple  
464 low-level features that compose an object across spatial and temporal scales (Brincat and  
465 Connor, 2004; Dicarlo et al., 2012): visual object detectors match visual features across  
466 spatial scales (Freiwald and Tsao, 2010; Quiroga, 2012; Tsao et al., 2006) – for instance, a  
467 face is recognized based on individual elements and their spatial relation (Freiwald et al.,  
468 2009). Likewise, acoustic object detectors match acoustic features across temporal scales  
469 (Gentner, 2008; Griffiths and Warren, 2004) – song detection neurons in the bird brain  
470 recognize the bird's own song by both syllable identity and sequence (Doupe and Konishi,  
471 1991; Gentner and Margoliash, 2003; Margoliash, 1983). pC2 neurons also bind different  
472 properties of the pulse song to selectively signal the presence of conspecific pulse song –  
473 pC2 is tuned to several features of pulse song like pulse carrier frequency, pulse duration,

474 inter-pulse interval, and pulse train duration and a match in only one feature is not sufficient  
475 to strongly drive these neurons (Fig. 3, S4A-C). They can therefore be considered acoustic  
476 object detectors.

477

478 ***Matches between behavioral tuning and conspecific song***

479 Behavioral selectivity for species-specific signals is thought to serve species separation. In  
480 FLyTRAP, locomotor tuning of *D. melanogaster* females overlaps with the conspecific song  
481 – females slow to conspecific song (Fig. 2A) and do not change their speed or may even  
482 accelerate for deviant pulse parameters (Fig. S2E). However, the tuning for any single song  
483 feature is not sufficiently narrow to serve as an effective filter for conspecific song. For  
484 instance, females also slow for IPIs produced by a sibling species *D. simulans* (50-65 ms)  
485 (Bennet-Clark and Ewing, 1969). However, *D. simulans* pulses would be rejected based on  
486 a mismatch in other song features – *D. simulans* pulses are too short and of too high  
487 frequency to be accepted by females (Clemens et al., 2017; Riabinina et al., 2011).

488 Selectivity for multiple song features may thus enable species discrimination with relatively  
489 broad single-feature tuning (Amézquita et al., 2011). In addition, males and females are  
490 exposed to additional non-acoustic cues during courtship that may further sharpen  
491 behavioral tuning. For instance, chemical cues prevent males from courting heterospecific  
492 females (Fan et al., 2013) and likely also contribute to female rejection (Billeter et al., 2009;  
493 Rybak et al., 2002b) – it will be interesting to explore how non-auditory cues (Keleman et al.,  
494 2012; Zhang et al., 2016) modulate locomotor responses to song and whether multi-modal  
495 integration occurs in pC2 neurons or elsewhere. The absence of non-acoustic cues may  
496 also explain the diversity of locomotor responses across strains in the FLyTRAP assay (Fig.  
497 S3). Using a naturalistic courtship assay, previous studies show that these same strains  
498 exhibit similar behaviors – males pattern their song in response to the female behavior and  
499 females change their locomotor speed to the natural courtship song similarly across all  
500 strains (Clemens et al., 2017; 2015; Coen et al., 2016; 2014).

501

502 In contrast to pulse song responses, the locomotor and singing responses for sine song  
503 were less sex-specific (Fig. 2E) and the behavioral tuning did not match well the conspecific  
504 song – very low frequencies never produced by males slowed females the most (Fig. 2A, B).  
505 This implies divergent roles for the two song modes and is consistent with previous studies  
506 (Eberl et al., 1997; F. V. Schilcher, 1976) – for instance sine song does not induce male-  
507 male courtship (Yoon et al., 2013). It has been suggested that pulse song may modulate

508 sine song responses (F. V. Schilcher, 1976) but we did not detect strong serial interactions  
509 between the two song modes (Fig. S2G). Alternatively, responses to sine song may depend  
510 more strongly on the presence of male chemical cues (Billeter et al., 2009; Kurtovic et al.,  
511 2007) that are absent in the FLyTRAP assay. This is consistent with sine song being  
512 produced when the male is near the female (Coen et al., 2014) – that is, when these  
513 chemical cues are particularly strong.

514

515 ***Pathways for detecting sine and pulse***

516 Our behavioral and neuronal results suggest that pulse and sine song are processed in  
517 parallel pathways (Fig. 2E, 3C, F-H) but it is unclear as of yet how and where sounds are  
518 split into different streams. Sine and pulse can be separated based on spectral and temporal  
519 properties (Fig. S5). In fact, the frequency tuning in auditory receptor neurons (JON) and  
520 first-order auditory brain neurons (AMMC) may already be sufficient to separate the lower-  
521 frequency sine (150Hz) from the higher-frequency pulse (>220Hz) (Azevedo and Wilson,  
522 2017; Ishikawa et al., 2017; Kamikouchi et al., 2009; Patella and Wilson, 2018; Yorozu et al.,  
523 2009). Temporal pattern could further discriminate pulse from sine by either suppressing  
524 responses to the sustained sine via adaptation or by tuning temporal integration such that  
525 the brief pulse stimuli fail to drive neuronal spiking. A complete mapping of auditory  
526 pathways and auditory activity throughout the *Drosophila* brain is required to identify where  
527 and how the neural selectivity for the different song modes arises.

528

529 Here, we have identified pC2 as one of the pathways driving responses to pulse song – pC2  
530 tuning matches the behavioral tuning for pulse song (Fig. 3G, H), pC2 activation drives sex-  
531 specific responses to song (Fig. 5), and experience-dependent modulation of pC2 tuning  
532 matches the behavioral tuning (Fig. 6). But, our data also indicate that it is not the only  
533 pathway used to detect pulse song – for example, we observed locomotor responses to  
534 pulse song even when pC2 neurons were silenced in females (Fig. 5M). Interestingly,  
535 previous studies have implied pC1 as a pulse song detector (Zhou et al., 2015; 2014). Like  
536 pC2, pC1 exists in males and females (Rideout et al., 2010), and activation drives several  
537 courtship-related behaviors in males – including singing, male-male courtship, or aggression  
538 (Koganezawa et al., 2016; Kohatsu et al., 2011; Pan et al., 2012; Philipsborn et al., 2011;  
539 Zhou et al., 2015) – and also in females (Li et al., 2018; Rezával et al., 2016; Zhou et al.,  
540 2014). All previous studies have relied on imaging activity in the lateral junction (LJ) to show  
541 that pC1 preferentially responds to pulse song (Zhou et al., 2015; 2014). However, we show

542 here that calcium responses of Dsx+ neurons in the LJ reflect the auditory activity of multiple  
543 Dsx+ cell types – and we detected auditory responses in the somata of pC2, pC1 (only in  
544 females) and pMN2 (only in females) (Fig. 4). Because the number of auditory neurons  
545 within the pC2 cluster is much larger than for pC1 or pMN2 (Fig. 4C), and because tuning in  
546 pC2 somas matches the tuning in the LJ (Fig. 4E-H), we conclude that the LJ activity largely  
547 reflects pC2 responses. Nonetheless, we have not exhaustively assessed the match  
548 between the neuronal responses of female pC1 and pMN2 neurons and behavior. Those  
549 neurons may also be critical for the female’s response to pulse song, including behaviors not  
550 investigated here (such as oviposition (Kimura et al., 2015)).

551

#### 552 ***Inputs and outputs of pC2 neurons***

553 How the selectivity of pC2 for pulse song arises is as of yet unclear since systematic studies  
554 of tuning for multiple pulse song features in the early auditory pathway are missing.  
555 However, existing evidence suggests that pC2 may acquire its feature selectivity in a serial  
556 manner – via a cumulative sharpening of tuning for song features at successive stages of  
557 auditory processing (Kamikouchi et al., 2009; Yamada et al., 2018; Zhou et al., 2015; 2014).  
558 Auditory receptor neurons display diverse and specific band-pass tuning for carrier  
559 frequency (Ishikawa et al., 2017; Kamikouchi et al., 2009; Patella and Wilson, 2018; Yorozu  
560 et al., 2009) and first order auditory B1 neurons further sharpen frequency tuning via  
561 resonant conductances (Azevedo and Wilson, 2017). Likewise, peripheral responses are  
562 already weakly tuned for IPI (Clemens et al., 2018; Ishikawa et al., 2017) and this tuning is  
563 further sharpened in downstream neurons (Vaughan et al., 2014; Zhou et al., 2015) through  
564 the interplay of excitation and inhibition (Yamada et al., 2018). This serial sharpening is  
565 similar to how selectivity for pulse song arises in crickets, in which a delay-line and  
566 coincidence detector mechanism produces broad selectivity for pulse duration and pulse  
567 pause which is subsequently sharpened in a downstream neuron (Schöneich et al., 2015).  
568 More direct readouts of the membrane voltage of auditory neurons in the fly brain are  
569 required to determine the biophysical mechanisms that generate song selectivity in pC2.

570

571 Similarly, the circuits downstream of pC2 neurons that control the diverse and sex-specific  
572 behaviors reported here remain to be identified. pC2 neurons may connect directly with  
573 descending interneurons (DNs) (Cande et al., 2017; Namiki et al., 2017) that control motor  
574 behaviors. For example, pC2 activation in males drives pulse song production, followed by  
575 sine song production at stimulus offset (Fig. 5A). This behavior resembles that caused by

576 pIP10 activation (Clemens et al., 2017) – pIP10 is a sex-specific descending neuron  
577 (Philipsborn et al., 2011), but we don't yet know if it directly connects with pC2 neurons. The  
578 fact that song responses are bi-directional – pulse song can induce both slowing and  
579 acceleration within each sex (Fig. 2A, B, S2) – implies that the sex-specificity of motor  
580 control is more than a simple re-routing from accelerating DNs in males to slowing DNs in  
581 females. Notably, song also promotes copulation, but we did not detect a significant effect of  
582 pC2 inactivation on copulation rates (Fig. S6I). This could be because our driver only labeled  
583 1/3 of the auditory pC2 neurons or because pC2 activity does not inform the decision to  
584 mate. That is, there may exist parallel pathways that control song responses on different  
585 timescales: one pathway that accumulates song information over timescales of minutes  
586 (Clemens et al., 2015; Ratcliff et al., 2016) and ultimately controls the mating decision while  
587 another, independent pathway controls behavioral responses to song on sub-second  
588 timescales, such as dynamic adjustments in locomotion and the production of courtship  
589 song.  
590

591 ***Modularity facilitates plasticity of behavioral responses to song***  
592 Our behavioral data strongly suggest that the sex-specificity of behavior arises after feature  
593 tuning – that is, the shared object detector – pC2 – determines the magnitude of behavioral  
594 responses in both sexes (Fig. 3G, H), and sex-specific aspects, such as the sign and  
595 dynamics of locomotor responses or singing in males, are driven by sex-specific circuits  
596 downstream of pC2 (Fig. 5). This is reminiscent of how sex-specific behaviors are driven to  
597 the male pheromone cVA in flies: shared detector neurons – olfactory receptor neurons and  
598 projection neurons in the antennal lobe – detect cVA in both sexes, and this information is  
599 then routed to sex-specific higher-order neurons in the lateral horn, which are thought to  
600 drive the different behaviors (Datta et al., 2008; Kohl et al., 2013; Ruta et al., 2010). This  
601 modular architecture with object detectors being flexibly routed to different behavioral  
602 outputs is beneficial if these routes are plastic. For instance, here we show that social  
603 experience can shape male responses to song (similar to (Li et al., 2018)), along with tuning  
604 at the level of the object detector neurons (Fig. 6). During mating, males transfer a sex  
605 peptide to females (Yapici et al., 2008) that alters female behavioral responses to song from  
606 slowing to acceleration (Coen et al., 2014) – these effects may be mediated at the level of  
607 the motor circuits downstream of pC2, shifting pulse song responses in females to resemble  
608 those of males. Modularity also facilitates behavioral plasticity on evolutionary time scales  
609 since only one element – the feature detector – needs to change for behavioral tuning in

610 both sexes to adapt to new songs that evolve during speciation (Capranica et al., 1973;  
611 Kostarakos et al., 2009). The identification of pC2 neurons as the pulse object detectors is  
612 therefore likely to benefit future studies of the evolution of song recognition.

613

614 ***pC2 neurons have a dual sensory and motor role***

615 Strikingly, our results imply a dual sensory and motor role of pC2 neurons: they drive the  
616 production of the sensory object they detect (Fig. 3F, G, 5A-C). This dual role may guide  
617 social interactions and communication via imitation. In *Drosophila melanogaster*, hearing the  
618 song of other males induces a male to court and sing to other females and even males  
619 (Eberl et al., 1997; Yoon et al., 2013). This behavior may have originated because the song  
620 of another male indicates the presence of a female nearby. pC2 is thus reminiscent of  
621 sensorimotor correspondence neurons found in vertebrates (Mooney, 2014; Prather et al.,  
622 2008; Rizzolatti and Fogassi, 2014) – neurons that are active during the production as well  
623 as the observation of a behavior. Such neurons are hypothesized to play a role in learning  
624 (Mooney, 2014) or – as is probably the case in *Drosophila* – imitation and communication  
625 between conspecifics (Rizzolatti and Arbib, 1998). However, pC2 differs crucially from these  
626 instances of “mirror” neurons in that it directly drives the production of the acoustic object it  
627 detects (Fig. 5A-C), while other sensorimotor correspondence neurons are activated by both  
628 sensory and motor-like inputs, but do not drive the object production itself. Because we  
629 recorded pC2 activity in passively listening males, we do not yet know whether pC2 is  
630 activated by sound in an actively singing male. If so, hearing its own song could induce self-  
631 stimulation and form a positive feedback loop to maintain courtship behavior by mediating  
632 persistent behavioral state-changes (Hoopfer et al., 2016). Alternatively, auditory inputs  
633 could be suppressed during singing via a corollary discharge (Poulet and Hedwig, 2003;  
634 Schneider et al., 2014), which would allow pC2 to maintain sensitivity to the song of other  
635 males to coordinate inter-male competition during singing. Additional studies of pC2 activity  
636 in behaving animals are required to fully understand how these pulse song detector neurons  
637 integrate into the acoustic communication behavior.

638

639 In summary, we show how the circuits that recognize song to drive diverse and sex-specific  
640 behavioral responses are organized in *Drosophila*: common detector neurons – pC2 –  
641 recognize pulse song in both males and females, and this identically processed information  
642 is then routed to drive multiple sex-specific behaviors. Similar principles may underlie the

643 production of sex-specific behavioral responses to acoustic communication signals in other  
644 insects, song birds or mammals.

645

646 **Acknowledgements:** Isabel D'Allesandro for help with playback behavioral experiments,  
647 Alex Hammons and Nofar Ozeri-Engelhard for help with dissections for immunostaining,  
648 Georgia Guan for help with crosses, immunostaining, and general technical assistance,  
649 Diego Pacheco for help with aligning the volumetric GCaMP scans, Robert Court and Doug  
650 Armstrong (<http://www.virtualflybrain.org>) for help with brain registration, David Stern, Ben  
651 Arthur and Barry Dickson for discussions during the development of the FLyTRAP assay,  
652 and Kai Feng and Barry Dickson for sharing the design of their playback assay chamber,  
653 Bruce Baker, Stephen Goodwin, Gerry Rubin, Peter Andolfatto for gifts of flies, and Kristin  
654 Scott, Asif Ghazanfar, Tim Buschman, as well as Christa Baker, Frederic Römschied and  
655 other members of the Murthy lab for feedback on the manuscript.

656

657 **Funding:** JC was funded by a Princeton Sloan-Swartz postdoctoral fellowship and by an  
658 Emmy-Noether grant from the German Research Foundation (DFG CL 596/1-1). MM was  
659 funded by an NIH Director's New Innovator (DP2) award, an NSF CAREER award, and an  
660 HHMI Faculty Scholar award.

661

662 **Author contributions:** JC, DD, and MM designed the study; JC primarily built the acoustic  
663 playback assay and collected behavioral data, with contributions from DD, and DD primarily  
664 collected anatomical and calcium imaging data, with contributions from JC; ST designed and  
665 built the two-photon imaging microscope; JC and DD analyzed data; JC and MM wrote the  
666 manuscript, with contributions from DD.

667

668 **References**

- 669 Amézquita, A., Flechas, S.V., Lima, A.P., Gasser, H., Hödl, W., 2011. Acoustic interference  
670 and recognition space within a complex assemblage of dendrobatid frogs. *Proc Natl  
671 Acad Sci U S A* 108, 17058–17063. doi:10.1073/pnas.1104773108
- 672 Aranha, M.M., Herrmann, D., Cachitas, H., Neto-Silva, R.M., Dias, S., Vasconcelos, M.L.,  
673 2017. apterous Brain Neurons Control Receptivity to Male Courtship in *Drosophila*  
674 *Melanogaster* Females. *Sci Rep* 7, 46242. doi:10.1038/srep46242
- 675 Arthur, B.J., Sunayama-Morita, T., Coen, P., Murthy, M., Stern, D.L., 2013. Multi-channel  
676 acoustic recording and automated analysis of *Drosophila* courtship songs. *BMC Biol* 11,  
677 11. doi:10.1186/1741-7007-11-11
- 678 Azevedo, A.W., Wilson, R.I., 2017. Active Mechanisms of Vibration Encoding and Frequency  
679 Filtering in Central Mechanosensory Neurons. *Neuron* 1–25.  
680 doi:10.1016/j.neuron.2017.09.004
- 681 Bennet-Clark, H.C., Ewing, A.W., 1969. Pulse interval as a critical parameter in the courtship  
682 song of *Drosophila melanogaster*. *Animal Behaviour* 17, 755–759. doi:10.1016/S0003-  
683 3472(69)80023-0
- 684 Bennet-Clark, H.C., Ewing, A.W., 1967. Stimuli provided by Courtship of Male *Drosophila*  
685 *melanogaster*. *Nature* 215, 669–671. doi:10.1038/215669a0
- 686 Billeter, J.-C., Atallah, J., Krupp, J.J., Millar, J.G., Levine, J.D., 2009. Specialized cells tag  
687 sexual and species identity in *Drosophila melanogaster*. *Nature* 461, 987–991.  
688 doi:10.1038/nature08495
- 689 Billeter, J.-C., Levine, J.D., 2013. Who is he and what is he to you? Recognition in  
690 *Drosophila melanogaster*. *Current Opinion in Neurobiology* 23, 17–23.  
691 doi:10.1016/j.conb.2012.08.009
- 692 Bizley, J.K., Cohen, Y.E., 2013. The what, where and how of auditory-object perception.  
693 *Nature Reviews Neuroscience* 14, 693–707. doi:10.1038/nrn3565
- 694 Blankers, T., Hennig, R.M., Gray, D.A., 2015. Conservation of multivariate female  
695 preference functions and preference mechanisms in three species of trilling field  
696 crickets. *Journal of Evolutionary Biology* n/a–n/a. doi:10.1111/jeb.12599
- 697 Brincat, S.L., Connor, C.E., 2004. Underlying principles of visual shape selectivity in  
698 posterior inferotemporal cortex. *Nature neuroscience* 7, 880–886. doi:10.1038/nn1278
- 699 Bussell, J.J., Yapici, N., Zhang, S.X., Dickson, B.J., Vosshall, L.B., 2014. Abdominal-B  
700 Neurons Control *Drosophila* Virgin Female Receptivity. *Current Biology* 24, 1584–1595.  
701 doi:10.1016/j.cub.2014.06.011
- 702 Cachero, S., Ostrovsky, A.D., Yu, J.Y., Dickson, B.J., Jefferis, G.S.X.E., 2010. Sexual  
703 dimorphism in the fly brain. *Current biology : CB* 20, 1589–1601.  
704 doi:10.1016/j.cub.2010.07.045
- 705 Cande, J., Berman, G.J., Namiki, S., Qiu, J., Korff, W., Card, G., Shaevitz, J.W., Stern, D.L.,  
706 2017. Optogenetic dissection of descending behavioral control in *Drosophila*. *bioRxiv* 1–  
707 50. doi:10.1101/230128
- 708 Capranica, R.R., Frishkopf, L.S., Nevo, E., 1973. Encoding of Geographic Dialects in the  
709 Auditory System of the Cricket Frog. *Science* 182, 1272–1275.  
710 doi:10.1126/science.182.4118.1272
- 711 Chen, T.-W., Wardill, T.J., Sun, Y., Pulver, S.R., Renninger, S.L., Baohan, A., Schreiter,  
712 E.R., Kerr, R.A., Orger, M.B., Jayaraman, V., Looger, L.L., Svoboda, K., Kim, D.S.,  
713 2013. Ultrasensitive fluorescent proteins for imaging neuronal activity. *Nature* 499, 295–  
714 300. doi:10.1038/nature12354
- 715 Clemens, J., Coen, P., Roemschied, F., Pereira, T., Mazumder, D., Pacheco, D., Murthy, M.,  
716 2017. Discovery of a new song mode in *Drosophila* reveals hidden structure in the  
717 sensory and neural drivers of behavior. *bioRxiv* 221044. doi:10.1101/221044

- 718 Clemens, J., Girardin, C.C., Coen, P., Guan, X.-J., Dickson, B.J., Murthy, M., 2015.  
719 Connecting Neural Codes with Behavior in the Auditory System of Drosophila. *Neuron*  
720 87, 1332–1343. doi:10.1016/j.neuron.2015.08.014
- 721 Clemens, J., Hennig, R.M., 2013. Computational principles underlying the recognition of  
722 acoustic signals in insects. *Journal of Computational Neuroscience* 35, 75–85.  
723 doi:10.1007/s10827-013-0441-0
- 724 Clemens, J., Ozeri-Engelhard, N., Murthy, M., 2018. Fast intensity adaptation enhances the  
725 encoding of sound in Drosophila. *Nat Commun* 9, 134. doi:10.1038/s41467-017-02453-9
- 726 Clyne, J.D., Miesenböck, G., 2008. Sex-specific control and tuning of the pattern generator  
727 for courtship song in Drosophila. *Cell* 133, 354–363. doi:10.1016/j.cell.2008.01.050
- 728 Coen, P., Clemens, J., Weinstein, A.J., Pacheco, D.A., Deng, Y., Murthy, M., 2014. Dynamic  
729 sensory cues shape song structure in Drosophila. *Nature* 507, 233–237.  
730 doi:10.1038/nature13131
- 731 Coen, P., Xie, M., Clemens, J., Murthy, M., 2016. Sensorimotor Transformations Underlying  
732 Variability in Song Intensity during Drosophila Courtship. *Neuron* 89, 629–644.  
733 doi:10.1016/j.neuron.2015.12.035
- 734 Cook, R.M., 1973. Courtship processing in *Drosophila melanogaster*. II. An adaptation to  
735 selection for receptivity to wingless males. *Animal Behaviour* 21, 349–358.  
736 doi:10.1016/S0003-3472(73)80077-6
- 737 Crossley, S.A., Bennet-Clark, H.C., Evert, H.T., 1995. Courtship song components affect  
738 male and female Drosophila differently. *Animal Behaviour* 50, 827–839.  
739 doi:10.1016/0003-3472(95)80142-1
- 740 Datta, S.R., Vasconcelos, M.L., Ruta, V., Luo, S., Wong, A., Demir, E., Flores, J., Balonze,  
741 K., Dickson, B.J., Axel, R., 2008. The Drosophila pheromone cVA activates a sexually  
742 dimorphic neural circuit. *Nature* 452, 473–477. doi:10.1038/nature06808
- 743 Dicarlo, J.J., Zoccolan, D., Rust, N.C., 2012. How Does the Brain Solve Visual Object  
744 Recognition? *Neuron* 73, 415–434. doi:10.1016/j.neuron.2012.01.010
- 745 Doupe, A.J., Konishi, M., 1991. Song-selective auditory circuits in the vocal control system  
746 of the zebra finch. *Proceedings of the National Academy of Sciences of the United  
747 States of America* 88, 11339–11343.
- 748 Dulac, C., Wagner, S., 2006. Genetic Analysis of Brain Circuits Underlying Pheromone  
749 Signaling. *Annu. Rev. Genet.* 40, 449–467.  
750 doi:10.1146/annurev.genet.39.073003.093937
- 751 Eberl, D.F., Duyk, G.M., Perrimon, N., 1997. A genetic screen for mutations that disrupt an  
752 auditory response in *Drosophila melanogaster*. *Proceedings of the National Academy of  
753 Sciences of the United States of America* 94, 14837–14842.  
754 doi:10.1146/annurev.neuro.20.1.567
- 755 Ellis, L.B., Kessler, S., 1975. Differential posteclosion housing experiences and reproduction  
756 in *Drosophila*. *Animal Behaviour* 23, 949–952. doi:10.1016/0003-3472(75)90119-0
- 757 Fan, P., Manoli, D.S., Ahmed, O.M., Chen, Y., Agarwal, N., Kwong, S., Cai, A.G., Neitz, J.,  
758 Renslo, A., Baker, B.S., Shah, N.M., 2013. Genetic and Neural Mechanisms that Inhibit  
759 Drosophila from Mating with Other Species. *Cell* 154, 89–102.  
760 doi:10.1016/j.cell.2013.06.008
- 761 Fortune, E.S., Rodríguez, C., Li, D., Ball, G.F., Coleman, M.J., 2011. Neural mechanisms for  
762 the coordination of duet singing in wrens. *Science* 334, 666–670.  
763 doi:10.1126/science.1209867
- 764 Freiwald, W.A., Tsao, D.Y., 2010. Functional Compartmentalization and Viewpoint  
765 Generalization Within the Macaque Face-Processing System. *Science* 330, 845–851.  
766 doi:10.1126/science.1194908
- 767 Freiwald, W.A., Tsao, D.Y., Livingstone, M.S., 2009. A face feature space in the macaque  
768 temporal lobe. *Nature neuroscience* 12, 1187–1196. doi:10.1038/nn.2363

- 769 Gentner, T.Q., 2008. Temporal scales of auditory objects underlying birdsong vocal  
770 recognition. *The Journal of the Acoustical Society of America* 124, 1350–1359.  
771 doi:10.1121/1.2945705
- 772 Gentner, T.Q., Margoliash, D., 2003. Neuronal populations and single cells representing  
773 learned auditory objects. *Nature* 424, 669–674. doi:10.1038/nature01731
- 774 Gerhardt, C.H., Huber, F., 2002. *Acoustic Communication in Insects and Anurans*. University  
775 Of Chicago Press.
- 776 Griffiths, T.D., Warren, J.D., 2004. What is an auditory object? *Nature Reviews  
777 Neuroscience* 5, 887–892. doi:10.1038/nrn1538
- 778 Haga, S., Hattori, T., Sato, T., Sato, K., Matsuda, S., Kobayakawa, R., Sakano, H.,  
779 Yoshihara, Y., Kikusui, T., Touhara, K., 2010. The male mouse pheromone ESP1  
780 enhances female sexual receptive behaviour through a specific vomeronasal receptor.  
781 *Nature* 466, 118–122. doi:10.1038/nature09142
- 782 Helversen, von, D., Helversen, von, O., 1997. Recognition of sex in the acoustic  
783 communication of the grasshopper *Chorthippus biguttulus* (Orthoptera, Acrididae).  
784 *Journal of Comparative Physiology A: Neuroethology, Sensory, Neural, and Behavioral  
785 Physiology* 180, 373–386. doi:10.1007/s003590050056
- 786 Hennig, R.M., Blankers, T., Gray, D.A., 2016. Divergence in male cricket song and female  
787 preference functions in three allopatric sister species. *Journal of Comparative  
788 Physiology A: Neuroethology, Sensory, Neural, and Behavioral Physiology* 202, 347–  
789 360. doi:10.1007/s00359-016-1083-2
- 790 Hennig, R.M., Heller, K.-G., Clemens, J., 2014. Time and timing in the acoustic recognition  
791 system of crickets. *Frontiers in Physiology* 5. doi:10.3389/fphys.2014.00286
- 792 Hoopfer, E.D., Jung, Y., Inagaki, H.K., Rubin, G.M., Anderson, D.J., Ramaswami, M., 2016.  
793 P1 interneurons promote a persistent internal state that enhances inter-male aggression  
794 in *Drosophila*. *eLife* 4, e11346. doi:10.7554/eLife.11346
- 795 Ishii, K.K., Osakada, T., Mori, H., Miyasaka, N., Yoshihara, Y., Miyamichi, K., Touhara, K.,  
796 2017. A Labeled-Line Neural Circuit for Pheromone-Mediated Sexual Behaviors in Mice.  
797 *Neuron* 95, 123–137.e8. doi:10.1016/j.neuron.2017.05.038
- 798 Ishikawa, Y., Okamoto, N., Nakamura, M., Kim, H., Kamikouchi, A., 2017. Anatomic and  
799 Physiologic Heterogeneity of Subgroup-A Auditory Sensory Neurons in Fruit Flies. *Front.  
800 Neural Circuits* 11, 46. doi:10.3389/fncir.2017.00046
- 801 Ito, K., Shinomiya, K., Ito, M., Armstrong, J.D., Boyan, G., Hartenstein, V., Harzsch, S.,  
802 Heisenberg, M., Homberg, U., Jenett, A., Keshishian, H., Restifo, L.L., Rössler, W.,  
803 Simpson, J.H., Strausfeld, N.J., Strauss, R., Vosshall, L.B., 2014. A Systematic  
804 Nomenclature for the Insect Brain. *Neuron* 81, 755–765.  
805 doi:10.1016/j.neuron.2013.12.017
- 806 Kamikouchi, A., Inagaki, H.K., Effertz, T., Hendrich, O., Fiala, A., Göpfert, M.C., Ito, K.,  
807 2009. The neural basis of *Drosophila* gravity-sensing and hearing. *Nature* 458, 165–171.  
808 doi:10.1038/nature07810
- 809 Keleman, K., Vrontou, E., Krüttner, S., Yu, J.Y., Kurtovic-Kozaric, A., Dickson, B.J., 2012.  
810 Dopamine neurons modulate pheromone responses in *Drosophila* courtship learning.  
811 *Nature*. doi:10.1038/nature11345
- 812 Kelley, D.B., 2003. Sexually Dimorphic Behaviors.  
813 <http://dx.doi.org/10.1146/annurev.ne.11.030188.001301> 11, 225–251.
- 814 Kimura, K.-I., Sato, C., Koganezawa, M., Yamamoto, D., 2015. *Drosophila* Ovipositor  
815 Extension in Mating Behavior and Egg Deposition Involves Distinct Sets of Brain  
816 Interneurons. *PLoS ONE* 10, e0126445. doi:10.1371/journal.pone.0126445
- 817 Klaoetke, N.C., Murata, Y., Kim, S.S., Pulver, S.R., Birdsey-Benson, A., Cho, Y.K.,  
818 Morimoto, T.K., Chuong, A.S., Carpenter, E.J., Tian, Z., Wang, J., Xie, Y., Yan, Z.,  
819 Zhang, Y., Chow, B.Y., Surek, B., Melkonian, M., Jayaraman, V., Constantine-Paton, M.,

- 820 Wong, G.K.-S., Boyden, E.S., 2014. Independent optical excitation of distinct neural  
821 populations. *Nat. Methods* 11, 338–346. doi:10.1038/nmeth.2836
- 822 Koganezawa, M., Kimura, K.-I., Yamamoto, D., 2016. The Neural Circuitry that Functions as  
823 a Switch for Courtship versus Aggression in *Drosophila* Males. *Current Biology* 26,  
824 1395–1403. doi:10.1016/j.cub.2016.04.017
- 825 Kohatsu, S., Koganezawa, M., Yamamoto, D., 2011. Female contact activates male-specific  
826 interneurons that trigger stereotypic courtship behavior in *Drosophila*. *Neuron* 69, 498–  
827 508. doi:10.1016/j.neuron.2010.12.017
- 828 Kohatsu, S., Yamamoto, D., 2015. Visually induced initiation of *Drosophila* innate courtship-  
829 like following pursuit is mediated by central excitatory state. *Nat Commun* 6, 6457.  
830 doi:10.1038/ncomms7457
- 831 Kohl, J., Ostrovsky, A.D., Frechter, S., Jefferis, G.S.X.E., 2013. A Bidirectional Circuit Switch  
832 Reroutes Pheromone Signals in Male and Female Brains. *Cell* 155, 1610–1623.  
833 doi:10.1016/j.cell.2013.11.025
- 834 Konishi, M., 1985. Birdsong: From Behavior to Neuron. *Annu. Rev. Neurosci.* 8, 125–170.  
835 doi:10.1146/annurev.neuro.8.1.125
- 836 Kostarakos, K., Hennig, M.R., Römer, H., 2009. Two matched filters and the evolution of  
837 mating signals in four species of cricket. *Frontiers in Zoology* 6, 22. doi:10.1186/1742-  
838 9994-6-22
- 839 Kurtovic, A., Widmer, A., Dickson, B.J., 2007. A single class of olfactory neurons mediates  
840 behavioural responses to a *Drosophila* sex pheromone. *Nature* 446, 542–546.  
841 doi:10.1038/nature05672
- 842 Lehnert, B.P., Baker, A.E., Gaudry, Q., Chiang, A.-S., Wilson, R.I., 2013. Distinct Roles of  
843 TRP Channels in Auditory Transduction and Amplification in *Drosophila*. *Neuron* 77,  
844 115–128. doi:10.1016/j.neuron.2012.11.030
- 845 Li, X., Ishimoto, H., Kamikouchi, A., 2018. Auditory experience controls the maturation of  
846 song discrimination and sexual response in *Drosophila*. *eLife* 7, e34348.  
847 doi:10.7554/eLife.34348
- 848 Margoliash, D., 1983. Acoustic parameters underlying the responses of song-specific  
849 neurons in the white-crowned sparrow. *J. Neurosci.* 3, 1039–1057.
- 850 Marlin, B.J., Mitre, M., D'Amour, J.A., Chao, M.V., Froemke, R.C., 2015. Oxytocin enables  
851 maternal behaviour by balancing cortical inhibition. *Nature* 520, 499–504.  
852 doi:10.1038/nature14402
- 853 Mooney, R., 2014. Auditory–vocal mirroring in songbirds. *Philosophical Transactions of the*  
854 *Royal Society B: Biological Sciences* 369, 20130179–399. doi:10.1098/rstb.2013.0179
- 855 Namiki, S., Dickinson, M.H., Wong, A.M., Korff, W., Card, G.M., 2017. The functional  
856 organization of descending sensory-motor pathways in *Drosophila*. *bioRxiv* 231696.  
857 doi:10.1101/231696
- 858 Nern, A., Pfeiffer, B.D., Rubin, G.M., 2015. Optimized tools for multicolor stochastic labeling  
859 reveal diverse stereotyped cell arrangements in the fly visual system. *Proc Natl Acad Sci*  
860 *U S A* 112, E2967–76. doi:10.1073/pnas.1506763112
- 861 Pan, Y., Meissner, G.W., Baker, B.S., 2012. Joint control of *Drosophila* male courtship  
862 behavior by motion cues and activation of male-specific P1 neurons. *Proc Natl Acad Sci*  
863 *U S A* 109, 10065–10070. doi:10.1073/pnas.1207107109
- 864 Patella, P., Wilson, R.I., 2018. Functional Maps of Mechanosensory Features in the  
865 *Drosophila* Brain. *Current Biology* 0. doi:10.1016/j.cub.2018.02.074
- 866 Philipsborn, von, A.C., Liu, T., Yu, J.Y., Masser, C., Bidaye, S.S., Dickson, B.J., 2011.  
867 Neuronal control of *Drosophila* courtship song. *Neuron* 69, 509–522.  
868 doi:10.1016/j.neuron.2011.01.011

- 869 Poulet, J.F.A., Hedwig, B., 2003. Corollary discharge inhibition of ascending auditory  
870 neurons in the stridulating cricket. *The Journal of neuroscience : the official journal of*  
871 *the Society for Neuroscience* 23, 4717–4725.
- 872 Prather, J.F., Peters, S., Nowicki, S., Mooney, R., 2008. Precise auditory–vocal mirroring in  
873 neurons for learned vocal communication. *Nature* 451, 305–310.  
874 doi:10.1038/nature06492
- 875 Quiroga, R.Q., 2012. Concept cells: the building blocks of declarative memory functions.  
876 *Nature Reviews Neuroscience* 13, 587–597. doi:10.1038/nrn3251
- 877 Ratcliff, R., Smith, P.L., Brown, S.D., McKoon, G., 2016. Diffusion Decision Model: Current  
878 Issues and History. *Trends Cogn. Sci. (Regul. Ed.)* 20, 260–281.  
879 doi:10.1016/j.tics.2016.01.007
- 880 Remedios, R., Kennedy, A., Zelikowsky, M., Grewe, B.F., Schnitzer, M.J., Anderson, D.J.,  
881 2017. Social behaviour shapes hypothalamic neural ensemble representations of  
882 conspecific sex. *Nature* 550, 388–392. doi:10.1038/nature23885
- 883 Rezával, C., Pattnaik, S., Pavlou, H.J., Nojima, T., Brüggemeier, B., D’Souza, L.A.D.,  
884 Dweck, H.K.M., Goodwin, S.F., 2016. Activation of Latent Courtship Circuitry in the  
885 Brain of Drosophila Females Induces Male-like Behaviors. *Current Biology* 26, 2508–  
886 2515. doi:10.1016/j.cub.2016.07.021
- 887 Riabinina, O., Dai, M., Duke, T., Albert, J.T., 2011. Active process mediates species-specific  
888 tuning of Drosophila ears. *Current biology : CB* 21, 658–664.  
889 doi:10.1016/j.cub.2011.03.001
- 890 Rideout, E.J., Dornan, A.J., Neville, M.C., Eadie, S., Goodwin, S.F., 2010. Control of sexual  
891 differentiation and behavior by the doublesex gene in *Drosophila melanogaster*. *Nature*  
892 *neuroscience* 13, 458–466. doi:10.1038/nn.2515
- 893 Rizzolatti, G., Arbib, M.A., 1998. Language within our grasp. *Trends in Neurosciences* 21,  
894 188–194. doi:10.1016/S0166-2236(98)01260-0
- 895 Rizzolatti, G., Fogassi, L., 2014. The mirror mechanism: recent findings and perspectives.  
896 *Philosophical Transactions of the Royal Society B: Biological Sciences* 369, 20130420–  
897 20130420. doi:10.1098/rstb.2013.0420
- 898 Robinett, C.C., Vaughan, A.G., Knapp, J.M., Baker, B.S., 2010. Sex and the single cell. II.  
899 There is a time and place for sex. *PLoS Biology* 8, e1000365.  
900 doi:10.1371/journal.pbio.1000365.g009
- 901 Ronacher, B., Ronacher, B., Hennig, R.M., Clemens, J., 2014. Computational principles  
902 underlying recognition of acoustic signals in grasshoppers and crickets. *J Comp Physiol*  
903 A 201, 61–71. doi:10.1007/s00359-014-0946-7
- 904 Rosenthal, G.G., Ryan, M.J., 2011. Conflicting preferences within females: sexual selection  
905 versus species recognition. *Biol. Lett.* 7, 525–527. doi:10.1098/rsbl.2011.0027
- 906 Ruta, V., Datta, S.R., Vasconcelos, M.L., Freeland, J., Looger, L.L., Axel, R., 2010. A  
907 dimorphic pheromone circuit in *Drosophila* from sensory input to descending output.  
908 *Nature* 468, 686–690. doi:10.1038/nature09554
- 909 Ryan, M.J., Cummings, M.E., 2013. Perceptual Biases and Mate Choice. *Annu. Rev. Ecol.*  
910 *Evol. Syst.* 44, 437–459. doi:10.1146/annurev-ecolsys-110512-135901
- 911 Ryan, M.J., Phelps, S.M., Rand, A.S., 2001. How evolutionary history shapes recognition  
912 mechanisms. *Trends Cogn. Sci. (Regul. Ed.)* 5, 143–148.
- 913 Rybak, F., Aubin, T., Moulin, B., Jallon, J.-M., 2002a. Acoustic communication in *Drosophila*  
914 *melanogaster* courtship: Are pulse-and sine-song frequencies important for courtship  
915 success? *Canadian journal of zoology* 80, 987–996.
- 916 Rybak, F., Sureau, G., Aubin, T., 2002b. Functional coupling of acoustic and chemical  
917 signals in the courtship behaviour of the male *Drosophila melanogaster*. *Proc. R. Soc. B*  
918 269, 695–701. doi:10.1098/rspb.2001.1919

- 919 Schilcher, F.V., 1976. The function of pulse song and sine song in the courtship of  
920 *Drosophila melanogaster*. *Animal Behaviour* 24, 622–625.  
921 Schilcher, Von, F., 1976. The role of auditory stimuli in the courtship of *Drosophila*  
922 *melanogaster*. *Animal Behaviour* 24, 18–26. doi:10.1016/S0003-3472(76)80095-4  
923 Schneider, D.M., Nelson, A., Mooney, R., 2014. A synaptic and circuit basis for corollary  
924 discharge in the auditory cortex. *Nature*. doi:10.1038/nature13724  
925 Schöneich, S., Kostarakos, K., Hedwig, B., 2015. An auditory feature detection circuit for  
926 sound pattern recognition. *Science Advances* 1, e1500325–e1500325.  
927 doi:10.1126/sciadv.1500325  
928 Stowers, L., Logan, D.W., 2010. Sexual dimorphism in olfactory signaling. *Current Opinion in*  
929 *Neurobiology* 20, 770–775. doi:10.1016/j.conb.2010.08.015  
930 Sweeney, S.T., Broadie, K., Keane, J., Niemann, H., O'Kane, C.J., 1995. Targeted  
931 expression of tetanus toxin light chain in *Drosophila* specifically eliminates synaptic  
932 transmission and causes behavioral defects. *Neuron* 14, 341–351. doi:10.1016/0896-  
933 6273(95)90290-2  
934 Talyn, B.C., Dowse, H.B., 2004. The role of courtship song in sexual selection and species  
935 recognition by female *Drosophila melanogaster*. *Animal Behaviour* 68, 1165–1180.  
936 doi:10.1016/j.anbehav.2003.11.023  
937 Tompkins, L., Gross, A.C., Hall, J.C., Gailey, D.A., Siegel, R.W., 1982. The role of female  
938 movement in the sexual behavior of *Drosophila melanogaster*. *Behav Genet* 12, 295–  
939 307. doi:10.1007/BF01067849  
940 Tsao, D.Y., Freiwald, W.A., Tootell, R.B.H., Livingstone, M.S., 2006. A cortical region  
941 consisting entirely of face-selective cells. *Science (New York, N.Y.)* 311, 670–674.  
942 doi:10.1126/science.1119983  
943 Tsao, D.Y., Livingstone, M.S., 2008. Mechanisms of Face Perception. *Annu. Rev. Neurosci.*  
944 31, 411–437. doi:10.1146/annurev.neuro.30.051606.094238  
945 Vaughan, A.G., Zhou, C., Manoli, D.S., Baker, B.S., 2014. Neural Pathways for the  
946 Detection and Discrimination of Conspecific Song in *D. melanogaster*. *Current Biology*.  
947 doi:10.1016/j.cub.2014.03.048  
948 Wang, L., Anderson, D.J., 2010. Identification of an aggression-promoting pheromone and  
949 its receptor neurons in *Drosophila*. *Nature* 463, 227–231. doi:10.1038/nature08678  
950 Yamada, D., Ishimoto, H., Li, X., Kohashi, T., Ishikawa, Y., Kamikouchi, A., 2018.  
951 GABAergic Local Interneurons Shape Female Fruit Fly Response to Mating Songs. *J.*  
952 *Neurosci.* 38, 4329–4347. doi:10.1523/JNEUROSCI.3644-17.2018  
953 Yamamoto, D., Yamamoto, D., Koganezawa, M., Koganezawa, M., 2013. Genes and circuits  
954 of courtship behaviour in *Drosophila* males. *Nature Reviews Neuroscience* 14, 681–692.  
955 doi:10.1038/nrn3567  
956 Yang, C.F., Shah, N.M., 2014. Representing Sex in the Brain, One Module at a Time.  
957 *Neuron* 82, 261–278. doi:10.1016/j.neuron.2014.03.029  
958 Yapici, N., Kim, Y.J., Ribeiro, C., Dickson, B.J., 2008. A receptor that mediates the post-  
959 mating switch in *Drosophila* reproductive behaviour. *Nature*.  
960 Yoon, J., Matsuo, E., Yamada, D., Mizuno, H., Morimoto, T., Miyakawa, H., Kinoshita, S.,  
961 Ishimoto, H., Kamikouchi, A., 2013. Selectivity and Plasticity in a Sound-Evoked Male-  
962 Male Interaction in *Drosophila*. *PLoS ONE* 8, e74289. doi:10.1371/journal.pone.0074289  
963 Yorozu, S., Wong, A., Fischer, B.J., Dankert, H., Kernan, M.J., Kamikouchi, A., Ito, K.,  
964 Anderson, D.J., 2009. Distinct sensory representations of wind and near-field sound in  
965 the *Drosophila* brain. *Nature* 458, 201–205. doi:10.1038/nature07843  
966 Yu, J.Y., Kanai, M.I., Demir, E., Jefferis, G.S.X.E., Dickson, B.J., 2010. Cellular organization  
967 of the neural circuit that drives *Drosophila* courtship behavior. *Current biology : CB* 20,  
968 1602–1614. doi:10.1016/j.cub.2010.08.025

- 969 Zhang, S.X., Rogulja, D., Crickmore, M.A., 2016. Dopaminergic Circuitry Underlying Mating  
970 Drive. *Neuron* 91, 168–181. doi:10.1016/j.neuron.2016.05.020
- 971 Zhou, C., Franconville, R., Vaughan, A.G., Robinett, C.C., Jayaraman, V., Baker, B.S., 2015.  
972 Central neural circuitry mediating courtship song perception in male *Drosophila*. *eLife* 4,  
973 11. doi:10.7554/eLife.08477
- 974 Zhou, C., Pan, Y., Robinett, C.C., Meissner, G.W., Baker, B.S., 2014. Central Brain Neurons  
975 Expressing doublesex Regulate Female Receptivity in *Drosophila*. *Neuron* 83, 149–163.  
976 doi:10.1016/j.neuron.2014.05.038
- 977

## **Methods**

### **Flies**

The following fly lines were used in our study:

<b>Genotype</b>	<b>Figures</b>	<b>Source/comment</b>
<i>D. melanogaster</i> NM91	1, 2, 3G,H,I, 4H, S1, S2, S3A, S6B,C	gift from Peter Andolfatto
8 <i>D. melanogaster</i> strains CM07, CarM03, N30, NM91, TZ58, ZH23, ZW109, and Canton S (lab stock)	S3B	Canton S is a lab stock, the 7 other strains are a gift from Peter Andolfatto
UAS-20X-GCaMP6m,UAS-tdTomato;dsx-Gal4 (Chen et al., 2013; Rideout et al., 2010)	3B-I 4B-D, F-H S3A , S4,S5A-C, S6, S7	dsx-Gal4 is a gift from Stephan Goodwin
UAS-eGFPX2;dsx-Gal4 (Rideout et al., 2010)	3A	
UAS>STOP>CsChrimson.mVenus/LexAop-flp; dsx-LexA, 8LexAop2-flp/R42B01-Gal4 (Klapoetke et al., 2014; Zhou et al., 2015; 2014)	5A-L S6A-E	R42B01-Gal4 and dsx-LexA are gifts from Bruce Baker. Drives expression of csChrimson in pC2 neurons and in a few pCd1/pCd2 neurons
UAS-GCaMP6m, UAS-TdTom/+;R42B01-Gal4/+ (Chen et al., 2013; Zhou et al., 2015; 2014)	S6A, right	R42B01-Gal4 is a gift from Bruce Baker
UAS>STOP>csChrimson/LexAop-flp; dsx-LexA, 8LexAop-Flp/R41A01-Gal4 (Klapoetke et al., 2014; Zhou et al., 2014)	S6D	Used to control for pCd1 neurons in the R42B01-Dsx intersection
UAS>STOP>TNT/LexAop-flp; dsx-LexA/R42B01-Gal4 (Sweeney et al., 1995; Zhou et al., 2015; 2014)	5M-O S6F-H	Inhibit synaptic output of pC2 neurons in females during courtship
+/LexAop-flp; dsx-LexA/R42B01-Gal4 (Zhou et al., 2015; 2014)	5M-O S6F-H	Control for pC2 TNT females
R71G01.AD/UAS-myrGFP;dsx.DBD/+ (Pan et al., 2012)	4A (pC1)	R71G01.AD is a gift from Gerald Rubin, dsx.DBD is a gift from Stephen Goodwin
R57G10-flpG5/+; dsx-Gal4/10UAS>STOP>HA, 10UAS>STOP>V5,10UAS>STOP>FLAG (Nern et al., 2015; Rideout et al., 2010)	4A (pMN2), 4E, S5E	Bloomington #64088 crossed with ;;dsx-Gal4
R57G10-flpI/+; dsx-Gal4/10UAS>STOP>HA, 10UAS>STOP>V5,10UAS>STOP>FLAG (Nern et al., 2015; Rideout et al., 2010)	4A (pC2I), S5D	Bloomington #64087 crossed with ;;dsx-Gal4



## **FLyTRAP**

Fly behavior was recorded with PointGrey cameras (FL3-U3-13Y3M-C or FL3-U3-13E4C-C). Grey color frames with a resolution of 1280x960 pixels were acquired at 30 frames per second using custom written software in python and saved as compressed videos. Sound representation was controlled using custom software written in Matlab. The sound stimuli were converted to an analog voltage signal using a National Instruments DAQ card (PCIe-6343). The signal was then amplified by a Samson s-amp headphone amp and used to drive a speaker (HiVi F6 6-1/2" Bass/Midrange). Sound intensity was calibrated as in (Clemens et al., 2015) by converting the voltage of a calibrated microphone (placed where the fly chambers would be during an experiment) to sound intensity and adjusting the sound amplification to match the target intensity. Sound and video were synchronized by placing into the camera's field-of-view a 650nm LED whose brightness was controlled using a copy of the sound signal. The chamber consisted of an array of 12 small arenas (7 by 46 mm, made from red plastic) that was placed in front of the loudspeaker (Movie S1). The arena floor consisted of plastic mesh to let sound into the chamber and the top was covered with a thin, translucent plastic sheet. Flies were illuminated using a white LED back light from below and a desk lamp from above.

## **Playback experiments**

Virgin male and female flies were isolated within 6 hours of eclosion and aged for 3-7 days prior to the experiments. Flies were raised at low density on a 12:12 dark:light cycle, at 25°C and 60% humidity. Flies were introduced gently into the chamber using an aspirator. Recordings were performed at 25°C and timed to start within 60 minutes of the incubator lights switching on to catch the morning activity peak. Stimulus playback was block-randomized to ensure that all stimuli within a set occur at the same overall rate throughout the stimulus. The stimulus set (e.g. five pulse trains with different IPIs, see Supplemental Table 1 for a list of all stimulus sets) was repeated for the duration of the experiment (2 hours). Stimuli were interleaved by 60 seconds of silence to reduce crosstalk between responses to subsequent stimulus presentations.

## **Stimulus design**

Sound was generated at a sampling frequency of 10 kHz using custom Matlab scripts. Sine song stimuli were created as pure tones of the specified frequency and intensity (typically 5mm/s). Pulse song was generated by arranging Gabor wavelets in trains interleaved by a specified pause. The Gabor wavelets were built by modulating the amplitude of a short sinusoidal using a Gaussian:  $\exp(-t^2/(2\sigma^2)) \sin(2\pi f * t + \phi)$ , where  $f$  is the pulse carrier frequency,  $\phi$  is the phase of carrier, and  $\sigma$  is proportional to the pulse duration. The parameters for all stimuli used along with the behavioral responses obtained in FLyTRAP are listed in Supplemental Table 1.

## **Analysis of FLyTRAP data**

Fly positions were tracked using custom-written software. Briefly, the image background was estimated as the median of 500 frames spaced to cover the full video. Foreground pixels (corresponding to the fly body) were identified by thresholding the absolute values of the

difference between each frame and the background estimate. The fly center position was then taken as the median of the position of all foreground pixels in each chamber. The sequence of fly positions across video frames was then converted into a time series using the light onset frames of the synchronization LED (indicating sound onset) as a reference. From the position time series fly speed was calculated and the speed traces were then aligned to stimulus onset for each trial. Base line speed was calculated as the average of the speed over an interval starting 30 seconds and ending 2 seconds before stimulus onset. Test speed was calculated over an interval starting at stimulus onset and ending 2 seconds after stimulus offset. Tuning curves were calculated as the difference between baseline speed and test speed for each trial, averaged over trials for each stimulus and animal. Speed traces were obtained by subtracting the baseline speed from the trace for each trial and averaging over trials for each stimulus and animal. All data (tuning curves, speed traces) are presented as mean +/- s.e.m. over flies.

### **Manual scoring of wing extension in FLyTRAP**

To evaluate the number of flies that extend their wings upon playback of pulse or sine song, we manually scored wing extension in the videos using the VirtualDub software. For pulse song (see Movie S2), we scored 25 stimuli/fly, choosing trials randomly but ensuring that each IPI (16/36/56/76/96 ms) was scored 5 times/fly. To avoid bias, the scorer was blind to the IPI presented to the fly in each trial. A total of 120 male flies and 36 female flies were scored (3000 and 900 single-fly responses total for pulse song). We scored wing extension only when the wing was extended in the first 1/3 second following stimulus onset, and only when the wings were not extended during the 1 second before stimulus onset. For sine song (150Hz carrier frequency), 60 males fly were scored.

### **Joint tuning for pulse duration and pulse pause**

To visualize locomotor (Fig. S2E, F) and calcium (Fig. S4D,E) responses to pulse trains with different combinations of pulse duration and pulse pause we generated smooth surface plots using Matlab's "scatteredInterpolant" function with the interpolation mode set to "natural". The boundaries of the plots were set as follows: Pulse duration of zero corresponds to silence and the speed values were set to 0 since all speed traces are always base line subtracted. A pulse pause of zero corresponds to a continuous oscillation and we set the corresponding speed values to those obtained for a 4 second pure tone with a frequency of 250 Hz.

### **Measurement of song features from natural song data**

The inter-pulse interval (IPI) is given by the interval between the peaks of subsequent pulses in a pulse train. Pulse trains correspond to continuous sequences of pulses with IPIs smaller than 200ms. Measuring the pulse durations from natural song data is non-trivial since pulses vary in their shape and can be embedded in background noise. We quantified pulse duration by 1) calculating the envelope of each pulse using the Hilbert transform, 2) smoothing that envelope using a Gaussian window with a standard deviation of 2 ms, and 3) taking as the pulse duration the full width of the smoothed envelope at 20% of the maximum amplitude of the pulse. Pulse durations for artificial stimuli used in our pulse train were defined to be consistent with this method. Pulse carrier frequency is given by the center of mass of the amplitude spectrum of

each pulse (Clemens et al., 2017). Sine carrier frequency was calculated as the peak frequency of the power spectrum of individual sine tones.

### PCA of speed traces

For the PCA of sex-specific responses to sound and optogenetic activation of pC2 (Fig. 5L) we collected male and female speed traces for all IPIs (Fig. 5D, F) and optogenetic activation levels (Fig. 5H, J) into a large matrix. Each speed trace was cut to include only the 12 seconds after sound onset and then normalized to have zero mean and unit variance. The first two principal components explain 84% of the total data variance.

### Optogenetic experiments

CsChrimson was expressed in pC2 neurons using the intersection between R42B01-Gal4 and dsx-LexA. 655nm light was emitted from a ring of 6 Tri-Star LEDs (LuxeonStar, SinkPAD-II 20mm Tri-Star Base) in FLyTRAP (Fig. 5D-K). Flies were fed with food that contained all-trans retinal for a minimum of three days post eclosion. Control were raised on regular fly food after eclosion. The LED was on for four seconds with 60 seconds pause between stimuli, similar to the temporal pattern used for auditory stimulus delivery in FLyTRAP (1-5mW/cm<sup>2</sup>, 100Hz, duty cycle 0.5). To measure the amount of song driven by pC2 activation in solitary flies, we used a chamber whose floor was tiled with 16 microphones to allow recording of the song (Fig. 5A-C, Movie S7; see (Clemens et al., 2017)). The LED (627nm LEDs, LuxeonStar) was on for four seconds (frequency 25 Hz, duty cycle 0.5) and off for 60 seconds. We tested three different light intensities (1.8, 9, and 13 mW/cm<sup>2</sup>) that were presented in 3 blocks of 18 trials. The order of the three blocks (light intensities) was randomized for each fly. Fly song was segmented as described previously (Arthur et al., 2013; Coen et al., 2014).

### pC2 inactivation in females during courtship

Tetanus neurotoxin light chain (TNT) (Sweeney et al., 1995). was used to block synaptic transmission in pC2 neurons in females. 3-7 days old virgin males (wild type, NM91) and females (pC2-TNT: UAS>STOP>TNT/LexAop-flp; dsx-LexA/R42B01-Gal4, pC2-control: +/LexAop-flp; dsx-LexA/R42B01-Gal4) were paired in a custom-built chamber, designed to record fly song (~25 mm diameter, tiled with 16 microphones). Flies were allowed to interact for 30 minutes, and the percent of flies copulated as a function of time was scored (Fig. S6H). A monochrome camera (Point Grey, FL3-U3-13Y3M) was used to record the fly behavior at 60 frames per second. Fly position was tracked offline and song was segmented as previously described (Arthur et al., 2013; Coen et al., 2014). We then calculated song statistics (e.g. amount of song or number of pulses per window) and female locomotion (average female speed) in windows of 60s with 30s overlap (Clemens et al., 2015). For the rank correlations between male song features and female speed (Fig. 5M-O), we binned the female speed values into 16 bins with the bin edges chosen such that each bin was populated by an equal amount of samples (see Fig. 5M) and calculated the rank correlation between the binned female speed and the average male song feature per bin. Changes in correlation between control and experimental flies (Fig. 5O) were analyzed using an ANCOVA model with independent slopes

and intercepts. Significance was determined based on the p-value of the interaction term (model's genotype by song-feature) after Bonferroni correction.

### Calcium imaging

Imaging experiments were performed on a custom built two-photon laser scanning microscope equipped with 5mm galvanometer mirrors (Cambridge Technology), an electro-optic modulator (M350-80LA-02 KD\*P, Conoptics) to control the laser intensity, a piezoelectric focusing device (P-725, Physik Instrumente), a Chameleon Ultra II Ti:Sapphire laser (Coherent) and a water immersion objective (Olympus XLPlan 25X, NA=1.05). The fluorescence signal collected by the objective was reflected by a dichroic mirror (FF685 Dio2, Semrock), filtered using a multiphoton short-pass emission filter (FF01-680/sp-25, Semrock), split by a dichroic mirror (FF555 Dio3, Semrock) into two channels, green (FF02-525/40-25, Semrock) and red (FF01-593/40-25, Semrock), and detected by GaAsP photo-multiplier tubes (H10770PA-40, Hamamatsu). Laser power (measured at the sample plane) was restricted to 15 mW. The microscope was controlled in Matlab using ScanImage 5.1 (Vidrio). Single plane calcium signals (Fig. 3C-I, 4F,G and pMN2 neuron in Fig 4C-E) were scanned at 8.5 Hz (256X256 pixels). Pixel size was ~0.5µmX0.5µm when imaging the lateral junction or pC2l process and ~0.25µmX0.25µm when imaging cell bodies in a single plan (Fig 4G and pMN2 in Fig. 4B-D). For volumetric scanning of cell bodies (Figs 4B-D, S5A), volumes were acquired at 0.5Hz (256\*216, 20 planes, voxel size ~ 0.34µm X 0.4µm X 1.5µm), scanning one group of cells at a time (pC1, pC2, pCd).

After surgery (opening of the head capsule to reveal the brain), flies were placed beneath the objective and perfusion saline was continuously delivered directly to the meniscus. Sound playback was controlled using custom written Matlab software (Clemens et al., 2018). The software also stopped and started the calcium imaging via a TTL pulse sent to ScanImage (“external hardware trigger” mode). The sound stimulus was generated at a sampling rate of 10kHz and sent through an amplifier (Crown, D-75A) to a set of head phones (Koss, ‘The Plug’). A single ear plug was connected to one side of a plastic tube (outer-inner diameters 1/8”-1/16”) and the other tube tip was positioned 2 mm away from the fly arista. Sound intensity was calibrated by measuring the sound intensity 2 mm away from the tube tip with a pre-calibrated microphone at a range of frequencies (100Hz-800Hz) and the output signal was corrected according to the measured intensities. The pause between stimulus representation was 25 seconds. A stimulus set (26-36 stimuli) was presented to each fly for 3 times in block-randomized order as in the playback experiments. If the response decayed in the middle of a repetition (possibly because of drift in the z-axis), the whole repetition was discarded from the analysis. Typically, two full repetitions per fly were used for analysis.

Regions of interest (ROIs) for calcium response measurements (in the LJ, pC2 process and in single Dsx+ somata) were selected manually based on a z-projection of the tdTomato channel.  $\Delta F/F$  of the GCaMP signal was calculated as  $(F(t)-F_0)/F_0$ , where  $F_0$  is the mean fluorescence in the ROI in the 10 seconds preceding stimulus onset. Integral  $\Delta F/F$  (Fig. 3D, F-I) and peak  $\Delta F/F$

(Fig. 3F, inset) values were calculated in a window starting at sound stimulus onset and ending 25 seconds after sound stimulus offset. To compensate for differences in overall responsiveness across flies, we normalized  $\Delta F/F$  values of each fly by dividing the integral or peak  $\Delta F/F$  by the maximal value (of integral or peak  $\Delta F/F$ ) across all stimuli for that fly. For volumetric scanning (Fig. 4), each time series was first motion corrected using the rigid motion correction algorithm NoRMCorre (Pnevmatikakis and Giovannucci, 2017) using the tdTomato signal as the reference image.

### Light microscopy

Flies expressing GFP in Dsx+ neurons (UAS-eGFP2X; dsx-Gal4; Fig. 3A) and flies expressing CsChrimson.mVenus in pC2 neurons (R42B01-Gal4 intersected with dsx-LexA; Fig. S6) were immunostained and scanned in a confocal microscope. 2-4 day old flies were cold-anesthetized on ice, dissected in cold S2 insect medium (Sigma Aldrich, #S0146) and fixed for 30-40 minutes on a rotator at room temperature in 4% PFA in 0.3% PBTS (0.3% Triton in PBSX1), followed by 4x15 minutes washes in 0.3% PBTS and 30 minutes in blocking solution (5% normal goat serum in 0.3%PBTS). Brains were incubated over two nights at 4°C with primary antibody, washed with 0.3%PBT and incubated for two more nights at 4°C in secondary antibody, followed by washing (4x15 minutes in 0.3%PBTS and 4x20 minutes in PBS), and mounting with VestaShield for 2-7 days before imaging. Antibodies were diluted in blocking solution at the following concentrations: rabbit anti-GFP (Invitrogen #1828014; used against GFP and mVenus) 1:1000, mouse anti-Bruchpilot (nc82, DSHB AB2314866) 1:20, goat anti-rabbit Alexa Flour 488 (Invitrogen #1853312) 1:200, goat anti-mouse Alexa Flour 633 (Invitrogen #1906490) 1:200.

Stochastic labeling of Dsx+ neurons in the female brain (Fig 4A, E) was done using multi-color-flip-out (MCFO, (Nern et al., 2015)) with three different epitope tags (HA,V5,FLAG). We followed the JFRC FlyLight Protocol ‘IHC-MCFO’ (<https://www.janelia.org/project-team/flylight/protocols>) for the preparation of brains. Flp was induced using R5710C10 promotor-coding sequence fusions of the flpG5 and flpl. Flies were 4-7 days old when dissected. Flies were stored at 25°C. Confocal stacks were acquired with a white light laser confocal microscope (Leica TCS SP8 X) and a Leica objective (HC PL APO 20x/0.75 CS2). A high-resolution scan of a pC2 cell (Fig 4E) was performed with an oil immersion Leica objective (HC PL APO 63x/1.40 Oil CS2, fig 4E). Images were registered to the Janelia brain template (JFRC2) (Jenett et al., 2012) using vfbaligner (<http://vfbaligner.inf.ed.ac.uk>), which internally uses CMTK for registration (Rohlfing and Maurer, 2003). The images of the fly brain in Figs 4A and S5D were deposited by G. Jefferis (Jefferis, 2014). Image processing was performed in FIJI (Schindelin et al., 2012).

## References

- Arthur, B.J., Sunayama-Morita, T., Coen, P., Murthy, M., Stern, D.L., 2013. Multi-channel acoustic recording and automated analysis of *Drosophila* courtship songs. *BMC Biol* 11, 11. doi:10.1186/1741-7007-11-11
- Chen, T.-W., Wardill, T.J., Sun, Y., Pulver, S.R., Renninger, S.L., Baohan, A., Schreiter, E.R., Kerr, R.A., Orger, M.B., Jayaraman, V., Looger, L.L., Svoboda, K., Kim, D.S., 2013. Ultrasensitive fluorescent proteins for imaging neuronal activity. *Nature* 499, 295–300. doi:10.1038/nature12354
- Clemens, J., Coen, P., Roemschied, F., Pereira, T., Mazumder, D., Pacheco, D., Murthy, M., 2017. Discovery of a new song mode in *Drosophila* reveals hidden structure in the sensory and neural drivers of behavior. *bioRxiv* 221044. doi:10.1101/221044
- Clemens, J., Girardin, C.C., Coen, P., Guan, X.-J., Dickson, B.J., Murthy, M., 2015. Connecting Neural Codes with Behavior in the Auditory System of *Drosophila*. *Neuron* 87, 1332–1343. doi:10.1016/j.neuron.2015.08.014
- Clemens, J., Ozeri-Engelhard, N., Murthy, M., 2018. Fast intensity adaptation enhances the encoding of sound in *Drosophila*. *Nat Commun* 9, 134. doi:10.1038/s41467-017-02453-9
- Coen, P., Clemens, J., Weinstein, A.J., Pacheco, D.A., Deng, Y., Murthy, M., 2014. Dynamic sensory cues shape song structure in *Drosophila*. *Nature* 507, 233–237. doi:10.1038/nature13131
- Jefferis, G.S.X.E., 2014. JFRC2 Template Brain. doi:10.5281/zenodo.10567
- Jenett, A., Rubin, G.M., Ngo, T.-T.B., Shepherd, D., Murphy, C., Dionne, H., Pfeiffer, B.D., Cavallaro, A., Hall, D., Jeter, J., Iyer, N., Fetter, D., Hausenfluck, J.H., Peng, H., Trautman, E.T., Svirskas, R.R., Myers, E.W., Iwinski, Z.R., Aso, Y., DePasquale, G.M., Enos, A., Hulamm, P., Lam, S.C.B., Li, H.-H., Laverty, T.R., Long, F., Qu, L., Murphy, S.D., Rokicki, K., Safford, T., Shaw, K., Simpson, J.H., Sowell, A., Tae, S., Yu, Y., Zugates, C.T., 2012. A GAL4-Driver Line Resource for *Drosophila* Neurobiology. *Cell Reports* 2, 991–1001. doi:10.1016/j.celrep.2012.09.011
- Klapoetke, N.C., Murata, Y., Kim, S.S., Pulver, S.R., Birdsey-Benson, A., Cho, Y.K., Morimoto, T.K., Chuong, A.S., Carpenter, E.J., Tian, Z., Wang, J., Xie, Y., Yan, Z., Zhang, Y., Chow, B.Y., Surek, B., Melkonian, M., Jayaraman, V., Constantine-Paton, M., Wong, G.K.-S., Boyden, E.S., 2014. Independent optical excitation of distinct neural populations. *Nat. Methods* 11, 338–346. doi:10.1038/nmeth.2836
- Nern, A., Pfeiffer, B.D., Rubin, G.M., 2015. Optimized tools for multicolor stochastic labeling reveal diverse stereotyped cell arrangements in the fly visual system. *Proc Natl Acad Sci U S A* 112, E2967–76. doi:10.1073/pnas.1506763112
- Pan, Y., Meissner, G.W., Baker, B.S., 2012. Joint control of *Drosophila* male courtship behavior by motion cues and activation of male-specific P1 neurons. *Proc Natl Acad Sci U S A* 109, 10065–10070. doi:10.1073/pnas.1207107109
- Pnevmatikakis, E.A., Giovannucci, A., 2017. NoRMCorre: An online algorithm for piecewise rigid motion correction of calcium imaging data. *Journal of Neuroscience Methods* 291, 83–94. doi:10.1016/j.jneumeth.2017.07.031
- Rideout, E.J., Dornan, A.J., Neville, M.C., Eadie, S., Goodwin, S.F., 2010. Control of sexual differentiation and behavior by the doublesex gene in *Drosophila melanogaster*. *Nature neuroscience* 13, 458–466. doi:10.1038/nn.2515
- Rohlfing, T., Maurer, C.R., 2003. Nonrigid image registration in shared-memory multiprocessor environments with application to brains, breasts, and bees. *IEEE Trans Inf Technol Biomed* 7, 16–25.

- Schindelin, J., Arganda-Carreras, I., Frise, E., Kaynig, V., Longair, M., Pietzsch, T., Preibisch, S., Rueden, C., Saalfeld, S., Schmid, B., Tinevez, J.-Y., White, D.J., Hartenstein, V., Eliceiri, K., Tomancak, P., Cardona, A., 2012. Fiji: an open-source platform for biological-image analysis. *Nat. Methods* 9, 676–682. doi:10.1038/nmeth.2019
- Sweeney, S.T., Broadie, K., Keane, J., Niemann, H., O'Kane, C.J., 1995. Targeted expression of tetanus toxin light chain in *Drosophila* specifically eliminates synaptic transmission and causes behavioral defects. *Neuron* 14, 341–351. doi:10.1016/0896-6273(95)90290-2
- Zhou, C., Franconville, R., Vaughan, A.G., Robinett, C.C., Jayaraman, V., Baker, B.S., 2015. Central neural circuitry mediating courtship song perception in male *Drosophila*. *eLife* 4, 11. doi:10.7554/eLife.08477
- Zhou, C., Pan, Y., Robinett, C.C., Meissner, G.W., Baker, B.S., 2014. Central Brain Neurons Expressing doublesex Regulate Female Receptivity in *Drosophila*. *Neuron* 83, 149–163. doi:10.1016/j.neuron.2014.05.038

**Figure 1**

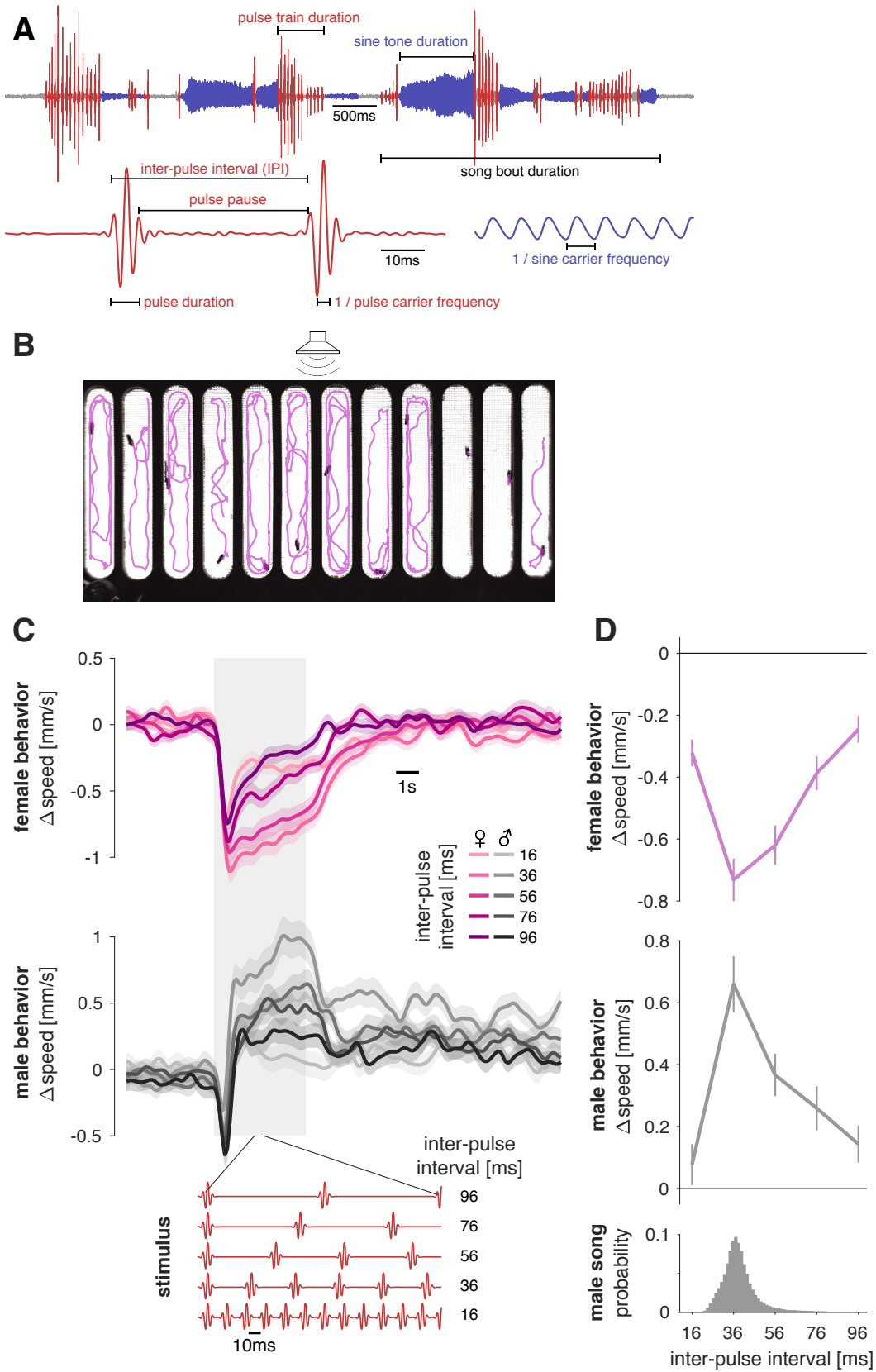


**Figure 1 – FLyTRAP assay for comparing locomotor tuning for courtship song stimuli in males and females.**

**A** *Drosophila melanogaster* produces song in bouts that can consist of two modes: Sine song corresponds to a weakly amplitude modulated oscillation with a species-specific carrier frequency (~150Hz) and pulse song corresponds to trains of Gabor-like wavelets each with a carrier frequency between 220 and 450Hz and a duration between 6 and 12 ms. These pulses are produced at an inter-pulse interval (IPI) of 30-45 ms.

**B** FLyTRAP consists of behavioral chamber that is placed in front of a speaker through which sound is presented. Fly movement is tracked using a camera. Shown is a single video frame of females in the assay with fly tracks for the preceding 20 seconds overlaid in magenta. See Movie S1.

**C** Locomotor responses of females (magenta) and males (grey) for pulse trains with different IPIs (see legend). The gray shaded box indicates the duration of the sound stimulus. Red traces at the bottom of the plot show short snippets of the 5 IPI stimuli presented in this experiment. Baseline speed was subtracted before trial averaging.

**D** Speed tuning curves for different IPIs in females (magenta) and males (grey) are obtained by averaging the speed traces in the six seconds following stimulus onset. The histograms at bottom shows the IPI distribution found in male song (data from 47 males of NM91 wild type strain totaling 82643 pulses).

Lines and shaded areas or error bars in C and D correspond to the mean  $\pm$  s.e.m. across 112 male and 112 female flies.

See also Figure S1 and Movie S1.

**Figure 2**

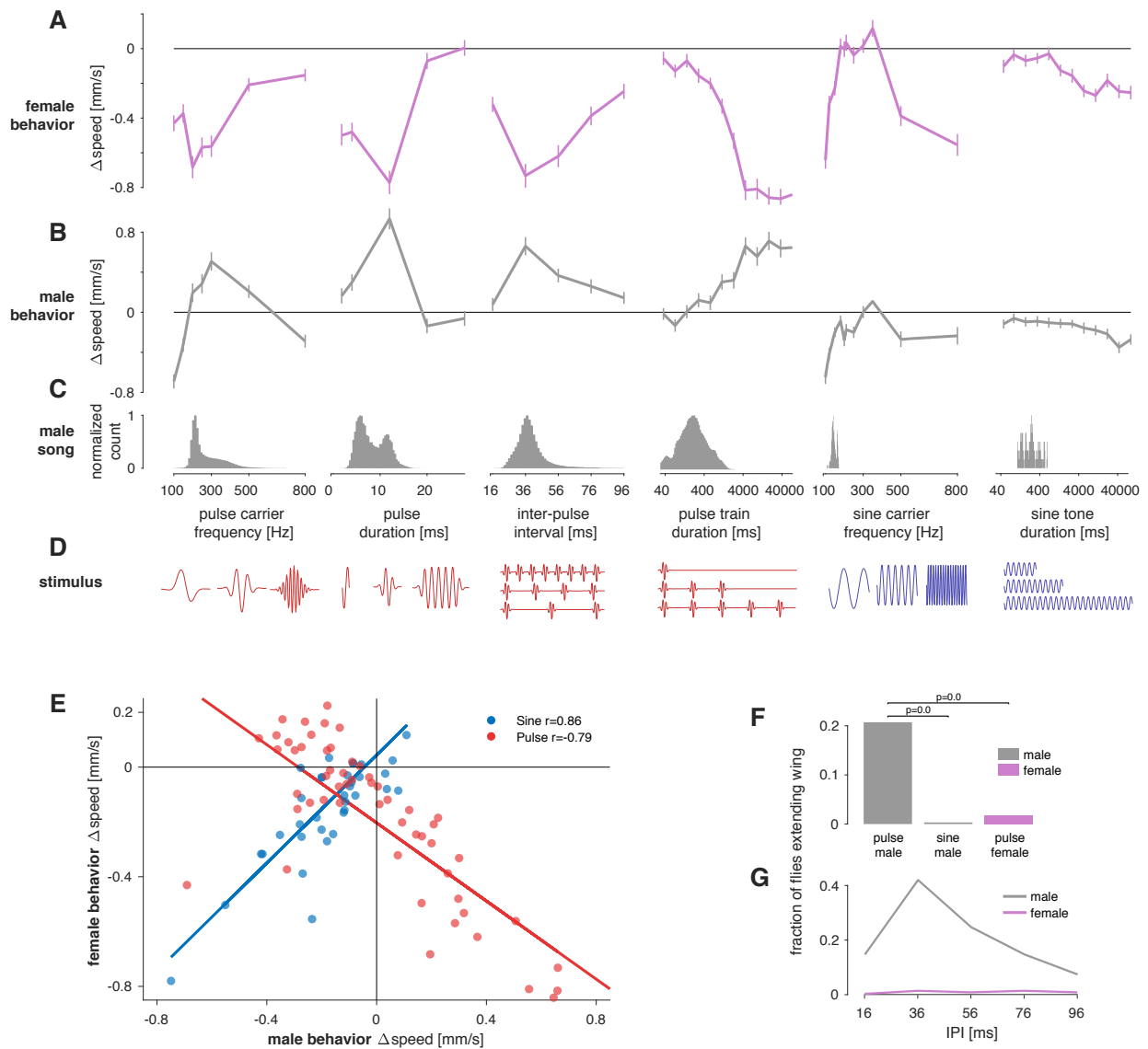


**Figure 2 – Responses to song playback are sex-specific and tuned for multiple features of pulse and sine song.**

**A, B** Locomotor tuning curves for females (A, magenta) and males (B, grey) for 6 different features of pulse and sine song. Lines and error bars correspond to the mean $\pm$ s.e.m. across flies (see Table S1 for a description of all stimuli and N flies).

**C** Distribution of the six different song features tested in A, B in the natural courtship song of *Drosophila melanogaster* males (data from 47 males of NM91 wild type strain totaling 82643 pulses and 51 minutes of sine song from 5269 song bouts). Histograms are normalized to a maximum of 1.0.

**D** Pictograms (not to scale) illustrating each song feature examined in A-C. Pulse and sine song features are marked red and blue, respectively.

**E** Changes in speed for males and females for all pulse (red) and sine (blue) stimuli tested (data from A, B, S2, see Table S1). Responses to sine stimuli are strongly and positively correlated between sexes ( $r=0.86$ ,  $p=4\times 10^{-7}$ ). Pulse responses are also strongly but negatively correlated ( $r=-0.79$ ,  $p=7\times 10^{-18}$ ). Blue and red lines correspond to linear fits to the responses to sine and pulse song, respectively.

**F** Fraction of trials for which male and female flies extended their wings during the playback of pulse song (five different IPIs as in 1C, D) and sine song (150Hz, quantified only for males). Solitary males (grey) frequently extend their wings in response to pulse but not to sine song. Solitary females (magenta) do not extend wings for pulse song. See also Movie S2.

**G** Fraction of trials that evoke wing extension in males (grey) and females (magenta) as a function of IPI. In males, wing extension and locomotor behavior (Figure 1D) exhibit strikingly similar tuning with a peak at the conspecific IPI. Females almost never extend their wing for any IPI.

See also Figure S2 and Movie S2.

**Figure 3**

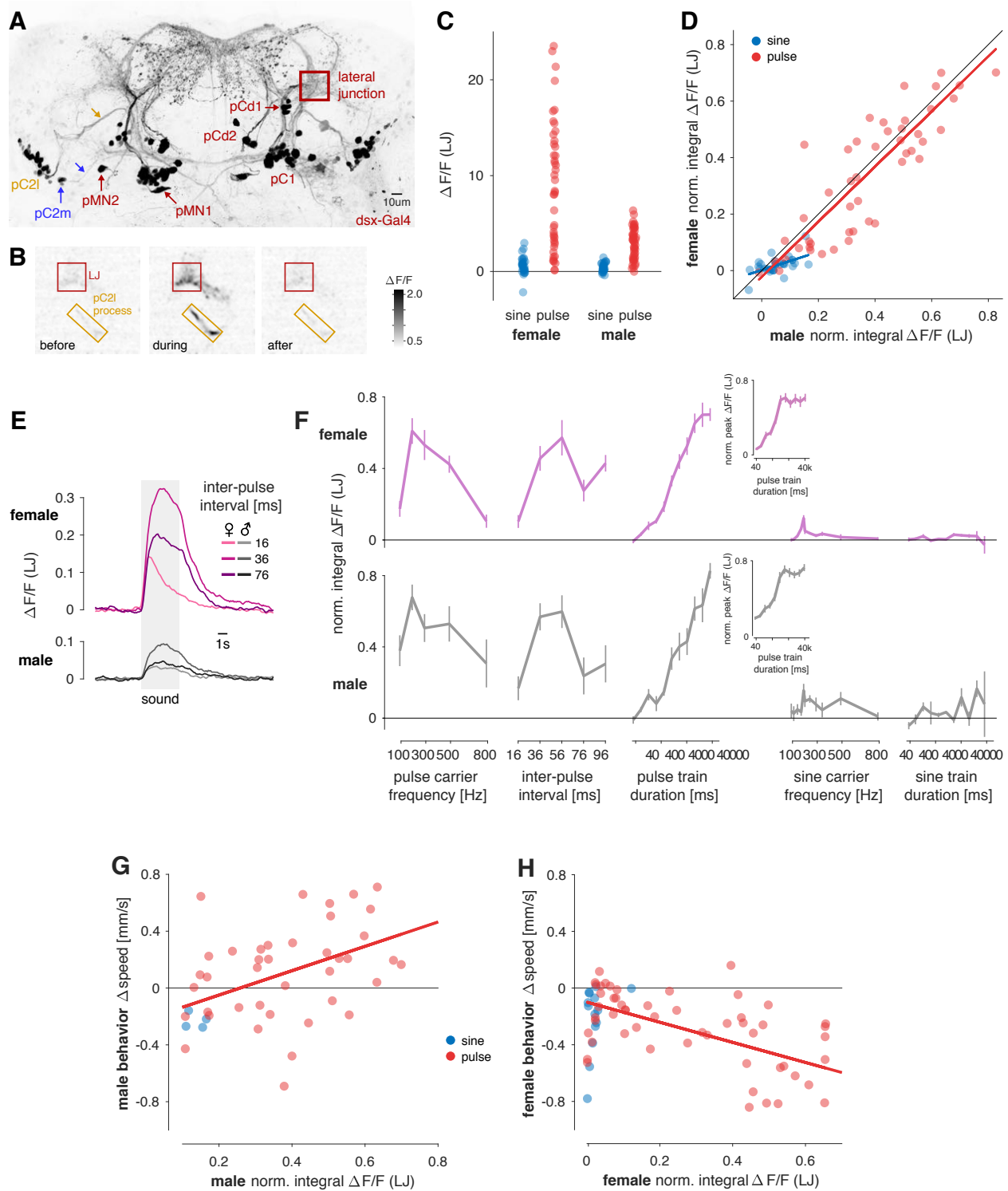


**Figure 3: Neuronal tuning in the LJ matches behavioral tuning for pulse stimuli in males and females.**

**A** Anatomy of Dsx+ neurons in the female brain. Max z-projection of a confocal stack of a fly brain in which all Dsx+ are labeled with GFP. 5/8 cell types (pC1, pC2I (yellow), pC2m (blue), pMN1, pMN2) project to the lateral junction (LJ), while 3 cell types (pCd1, pCd2, aDN (movie S11)) do not. Yellow and blue arrows point to the processes that connect pC2I and pC2m to the LJ. See also Fig. S5B,C.

**B** Grayscale image (see color bar) of calcium responses ( $\Delta F/F$ ) to a pulse train (IPI 36ms) in an ROI centered around the LJ (red) and the pC2I process (yellow) in a female. Shown are snapshots of the recording at three different time points relative to stimulus onset - before ( $T=-10s$ ), during ( $T=1.2s$ ), and after ( $T=20s$ ) the stimulus. Flies express GCaMP6m in all Dsx+ cells. Conspecific-like pulse elicits strong increases in fluorescence in the LJ and the pC2 process.

**C** LJ responses to sine (blue) and pulses (red) stimuli in females (left) and males (right). Individual dots correspond to integral  $\Delta F/F$  responses for individual stimuli averaged over the 3-12 individuals tested for each stimulus. Many pulse stimuli evoke much stronger responses than the most effective sine stimulus ( $p=8\times 10^{-11}$  for females and  $p=2\times 10^{-11}$  for males, two-sided rank sum comparison of sine and pulse responses).

**D** Comparison of male and female LJ responses to sine (blue) and pulse (red) stimuli. Responses to both song modes are correlated strongly for pulse ( $r^2=0.74$ ,  $p=3\times 10^{-15}$ ) and weakly for sine ( $r^2=0.31$ ,  $p=0.002$ ) stimuli. Individual dots correspond to the integral  $\Delta F/F$  for individual stimuli averaged across animals. Before averaging, the responses of each animal were normalized to compensate for inter-individual differences in calcium levels (see methods for details).

**E** Fluorescence traces from the LJ in females (top, magenta) and males (bottom, grey) for pulse trains with three different IPIs (see legend, average over 6 individuals for each sex). In both sexes, the LJ responds most strongly to the conspecific IPI of 36ms (Fig. 1D). Responses are much weaker for shorter (16ms) and longer (76ms) IPIs. Calcium responses in the LJ are smaller in males than in females (compare C). See also Supp. Movie S3, S4.

**F** Tuning curves of calcium responses in the female (magenta) and the male (gray) LJ for features of pulse and sine song (compare to behavioral tuning in Fig. 2A, B). Lines and error bars correspond to the mean $\pm$ s.e.m. across flies. Integral  $\Delta F/F$  normalized as in D. Insets show peak  $\Delta F/F$  tuning curves for pulse train duration. In contrast to the integral  $\Delta F/F$ , the peak  $\Delta F/F$  saturates for long pulse trains, indicating that the LJ stops accumulating calcium for pulse trains not normally produced by males. Apart from this difference, integral  $\Delta F/F$  and peak  $\Delta F/F$  are similar (see Fig. S4F, G).

**G, H** Comparison of behavioral and neuronal tuning in males (G) and females (H). Dots correspond to the average normalized integral  $\Delta F/F$  over individuals, lines indicate linear fits. In males (G), behavioral and neuronal responses are strongly and *positively* correlated for pulse (red,  $r=0.55$ ,  $p=9\times 10^{-6}$ ) but not for sine stimuli (blue,  $r=-0.15$ ,  $p=0.06$ ). In females (H), behavioral and neuronal responses are strongly and *negatively* correlated for pulse (red,  $r=-0.62$ ,  $p=2\times 10^{-7}$ ) but not for sine stimuli (blue,  $r=0.27$ ,  $p=0.30$ ). All  $\Delta F/F$  values are from flies expressing GCamp6m under the control of Dsx-Gal4. See also Figure S3 and S4, and Movie S3 and S4.

**Figure 4**

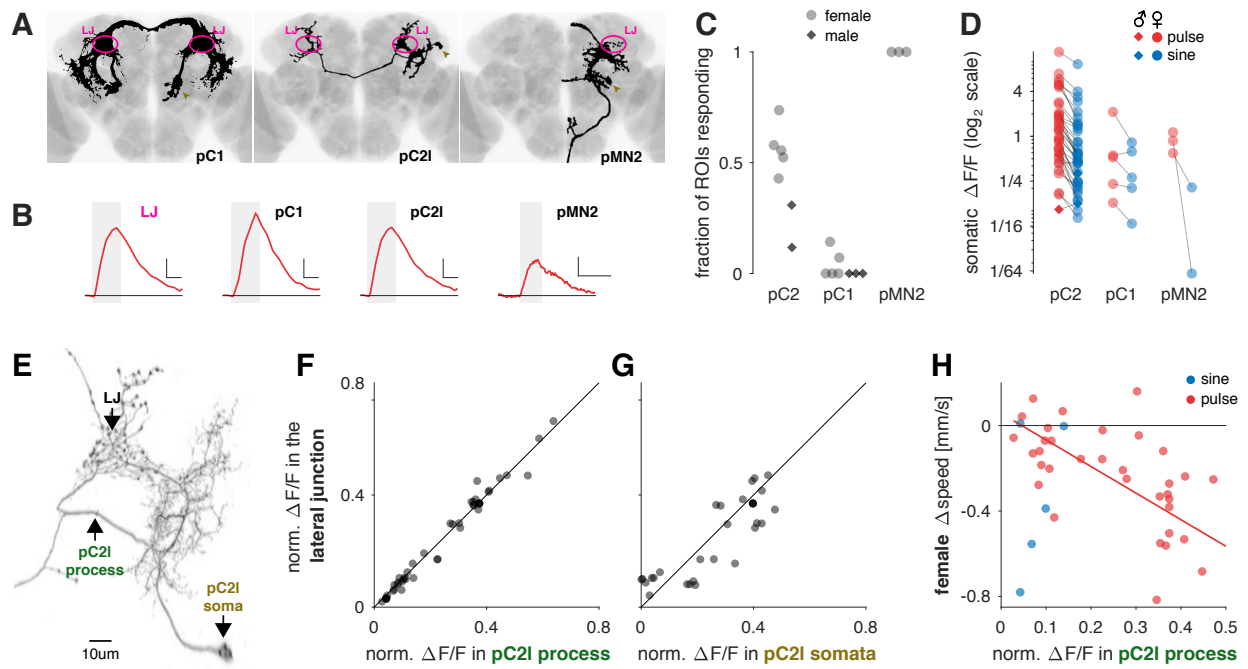


**Figure 4 - pC2 neurons are pulse object detectors common to both sexes.**

**A** Individual Dsx+ neuron types (black) with somas in the female central brain in which we detected calcium responses for pulse or sine song, registered to a common template brain (gray) (see Methods for details). Of the 8 Dsx+ cell types in the central brain, pC2l, pC2m, the single female-only neuron pMN2 and a small number of pC1 neurons (and only in some individuals) respond to courtship sounds. The lateral junction (LJ) is marked in magenta and somata are marked with golden arrow heads. See also Supp. Movie S10, S11.

**B** Example somatic fluorescence traces from single somata of the pC1, pC2, and pMN2 cells in response to pulse trains (IPI=36ms, single trial responses). Fluorescence trace from the LJ (magenta) shown for comparison. The gray box marks the duration of the sound stimulus. In each panel. Horizontal and vertical scale bars correspond to 6 seconds and 0.25 ΔF/F, respectively. Horizontal black line marks ΔF/F=0.

**C** Fraction of cells in Dsx+ clusters with detectable somatic calcium responses to pulse or sine song (females, light grey dots; males, dark grey squares). Complete clusters were imaged using volumetric scan for pC1, pC2 and single plane scans for pMN2. We did not distinguish between pC2l/m, since in most flies both groups are spatially intermingled at the level of cell bodies. Note that all flies included showed calcium responses to sound in the LJ, even when we did not detect responses in specific somata.

**D** Peak somatic ΔF/F for pulse (red) and sine (stimuli). Lines connect responses to pulse (36ms IPI) and sine (150Hz) recorded in the same animal. Note that responses are plotted on a log scale – the average of the ratio between sine and pulse for all cells is ~2.6. 36/38 pC2, 4/5 pC1 and 2/2 pMN2 prefer pulse over sine. See also Supp. Movie S5, S6.

**E** High resolution confocal scan of a single pC2l neuron (obtained via a stochastic labelling technique, see Methods for details). Only the side ipsilateral to the cell body is shown. The neurites in the lateral junction appear varicose, indicating that they contain pre-synaptic sites.

**F** Normalized integral ΔF/F values recorded simultaneously in the LJ and the process that connects the LJ with the somata of pC2l (and no other Dsx+ cell type) are highly correlated ( $r^2=0.99$ ,  $p=6\times 10^{-39}$ ). Each point corresponds to an individual stimulus (pulse or sine) averaged over flies ( $N=10-24$  flies per stimulus). The high correlation means that calcium responses in the LJ reflect responses in pC2l neurons.

**G** Normalized ΔF/F recorded first in the LJ and then in single pC2l somata in the same fly are highly correlated ( $r^2=0.81$ ,  $p=2\times 10^{-14}$ ,  $N=8$  flies per stimulus), demonstrating that calcium responses in the LJ represent the responses of individual pC2l cells, with some variability across individual cells and animals.

**H** Comparison of calcium responses pC2l process and female speed for the same stimuli. pC2l and behavioral responses are highly correlated for pulse but not for sine stimuli (pulse:  $r=-0.74$ ,  $p=3\times 10^{-7}$ , sine:  $r=0.44$ ,  $p=0.46$ ), just as for the LJ (compare Fig. 3H). The match between neuronal and behavioral tuning for pulse song indicates that pC2l neurons are pulse song detectors. Each point corresponds to an individual stimulus ( $\Delta$ speed:  $N\sim 120$  flies per stimulus,  $\Delta F/F$ :  $N=10-24$  flies per stimulus).

All ΔF/F values correspond to the integral fluorescence and are from flies expressing GCamp6m under the control of Dsx-Gal4. See also Figure S5 and Movie S5 and S6.

**Figure 5**

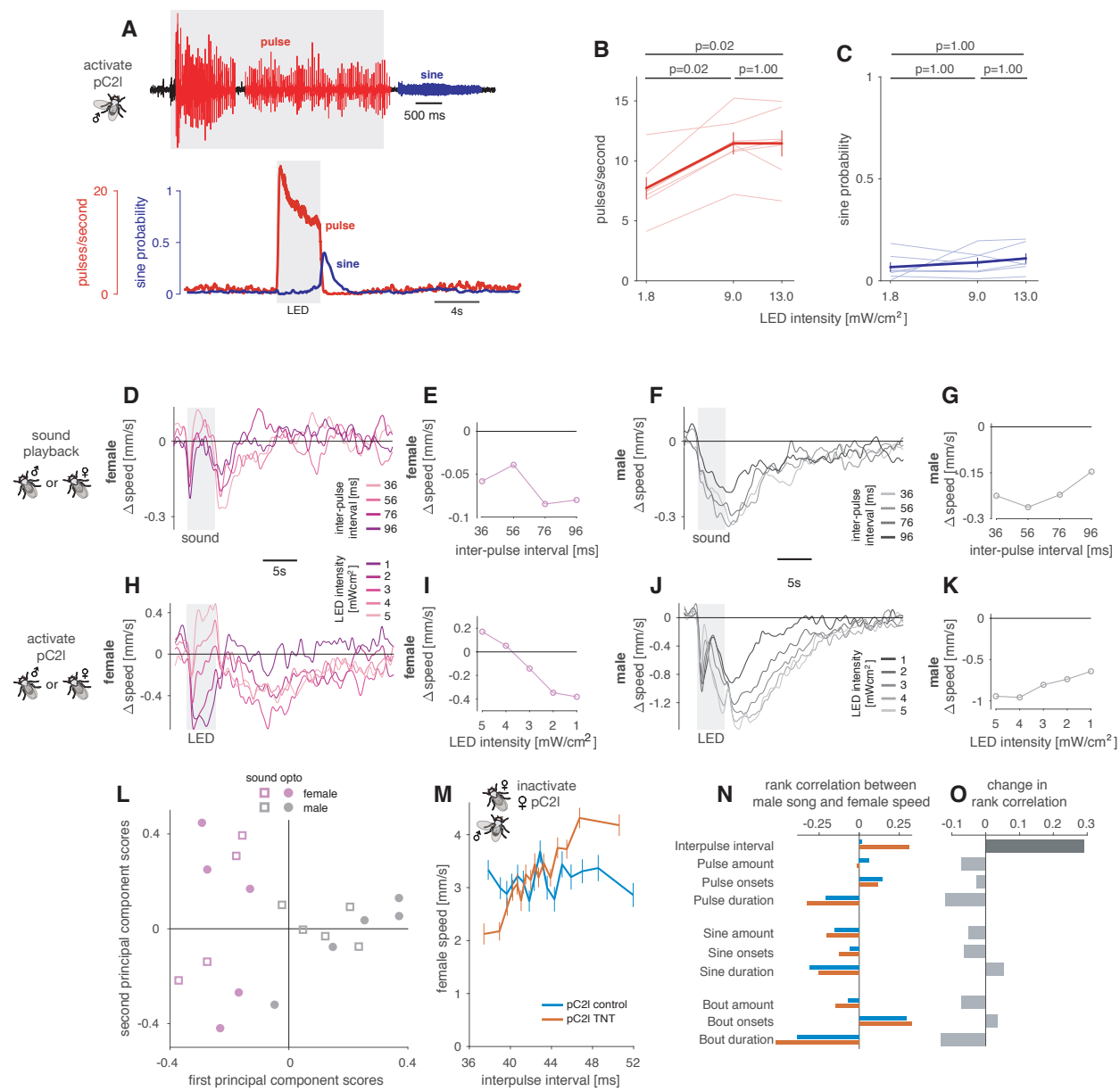


**Figure 5 – pC2 activation generates sex-specific behaviors.**

**A** Song evoked in males by optogenetic activation (627nm LEDs, intensity 13 mW/cm<sup>2</sup>) of a driver line that labels pC2I and pCd neurons (R42B01nDsx). Top trace shows a song recording marking pulse and sine song in red and blue, respectively. The grey area indicates the duration (4 seconds) of optogenetic activation. Pulse song is evoked during activation while sine song occurs immediately following activation. Bottom plots show pulse rate (red) and sine song probability (blue) averaged over 7 flies (18 stimulation epochs per animals). See also Movie S7.

**B, C** Average pulse rate (B) and sine song probability (C) evoked in the 6 seconds following LED light onset (LED duration is 4 seconds). Dose-response curves for individuals are shown as thin lines, population averages (mean±s.e.m.) are shown as thick lines with error bars. P-values result from two-sided sign tests and are adjusted for multiple comparisons using Bonferroni's method. Same data as in A. See also Supp. Movie S7, S8.

**D-G** Changes in speed in FLyTRAP for pulse trains (duration indicated by grey boxes) with different IPIs (see legend) in the R42B01nDsx strain. Female behavioral responses (magenta) were weak with multi-phasic dynamics (D, E). Males (grey) slowed for all pulse stimuli tested and responses outlast the stimulus duration (F, G). Data represent averages over 112 female and 113 male flies.

**H-K** Optogenetic activation of R42B01nDsx using csChrimson evokes locomotor responses with sex-specific dynamics. Changes in speed (grey box) and tuning curves were corrected for intrinsic light responses by subtracting the responses of control flies with the same genotype that were not fed retinal (see Fig. S6E). Females slow for weak and speed for strong activation with multi-phasic dynamics as for sound (H, I, compare D). Males decrease their speed and responses outlast the optogenetic stimulus as for sound (J, K, compare F). See also Supp. Movie S9. See S6E for N flies. The x scales of panels I, K are inverted to match the tuning for sound since the direction of the mapping between LED intensity and IPI is arbitrary.

**L** Principal component (PC) analysis of male and female locomotor speed traces (12s following stimulus LED or sound onset, traces taken from D, F, H, J). Shown are first and second principal component (PC) scores of females (magenta) and males (grey) for sound (squares) and optogenetic stimulation (circles). Female responses to different LED intensities and to different IPIs spread along the second PC while male responses to sound and optogenetic stimulation largely spread along the first PC.

**M** Locomotor tuning for IPI during natural courtship obtained from single females that were courted by a wild-type NM91 male. pC2I synaptic output in the females was inhibited using TNT using the R42B01nDsx driver. Lines and error bars correspond to the mean±s.e.m speed of N females per genotype tested (pC2I TNT – orange, pC2I control – blue, N=48 females for each genotype, see methods for details on how the tuning curves were computed). pC2I control females (blue) do not change their speed with IPI within the range commonly produced by males (rank correlation 0.02, p=0.59, compare Fig. 1D). pC2I TNT females (orange) accelerate for longer IPIs (rank correlation 0.31, p=3x10<sup>-30</sup>).

**N** Rank correlation between female speed and different song features during natural courtship (pC2I control – blue, pC2I TNT – orange).

**O** Difference between the rank correlations for control (blue) and pC2I TNT (orange) flies in N.

pC2I inactivation specifically changes the correlation between female speed and IPI (dark gray,  $p=6\times 10^{-8}$ ). All other changes in correlation are much smaller and not significant ( $p>0.18$ ). P-values were obtained by fitting an ANCOVA model (see methods for details) and were corrected for multiple comparisons using the Bonferroni method.

See also Figure S6 and Movie S7.

**Figure 6**

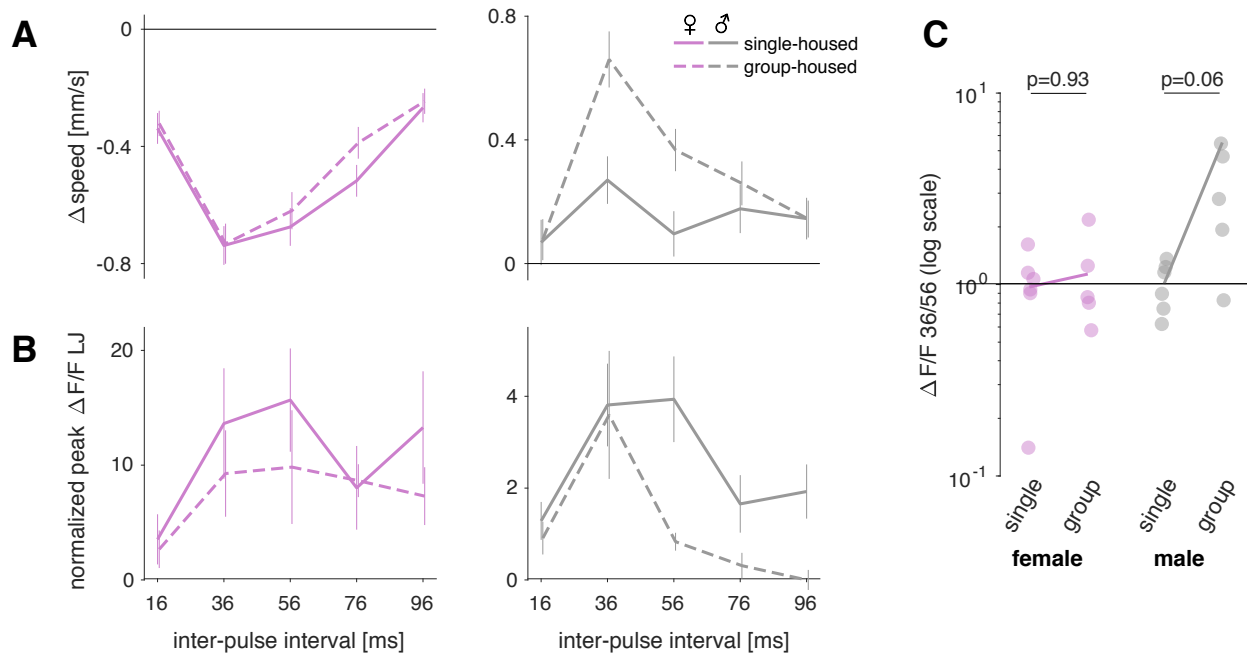


**Figure 6 – Locomotor and pC2 responses are similarly modulated by social experience.**

**A** Changes in speed for pulse trains measured using FLyTRAP with different IPIs in single-housed (solid line) or group-housed (dashed lines) female (left, magenta) and male flies (right, grey). Plots show mean  $\pm$  s.e.m. across 112 group-housed and 119 single-housed female or male flies. Female IPI tuning is not strongly affected by housing conditions. By contrast, males change their speed more strongly and more selectively when group-housed.

**B** Calcium responses from the LJ for pulse trains with different IPIs in single-housed (solid line) or group-housed (dashed lines) female (left, magenta) and male flies (right, grey). Plots show mean  $\pm$  s.e.m. across 5-6 female or male flies in each condition. In females, group housing only weakly suppresses LJ responses for some IPIs. By contrast, male LJ responses are selectively suppressed for long IPIs, which sharpens the IPI tuning.

**C** Ratio of Calcium responses to 36 and 56 ms IPIs in single-housed or group-housed female (left, magenta) and male flies (right, grey). Individual dots correspond to individual flies, the solid lines connect the population average ratios. P-values were obtained from a two-sided rank sum test.

All  $\Delta F/F$  values correspond to the integral fluorescence and are from flies expressing GCamp6m under the control of Dsx-Gal4.

See also Figure S7.

## Supplemental Figures

**Figure S1**

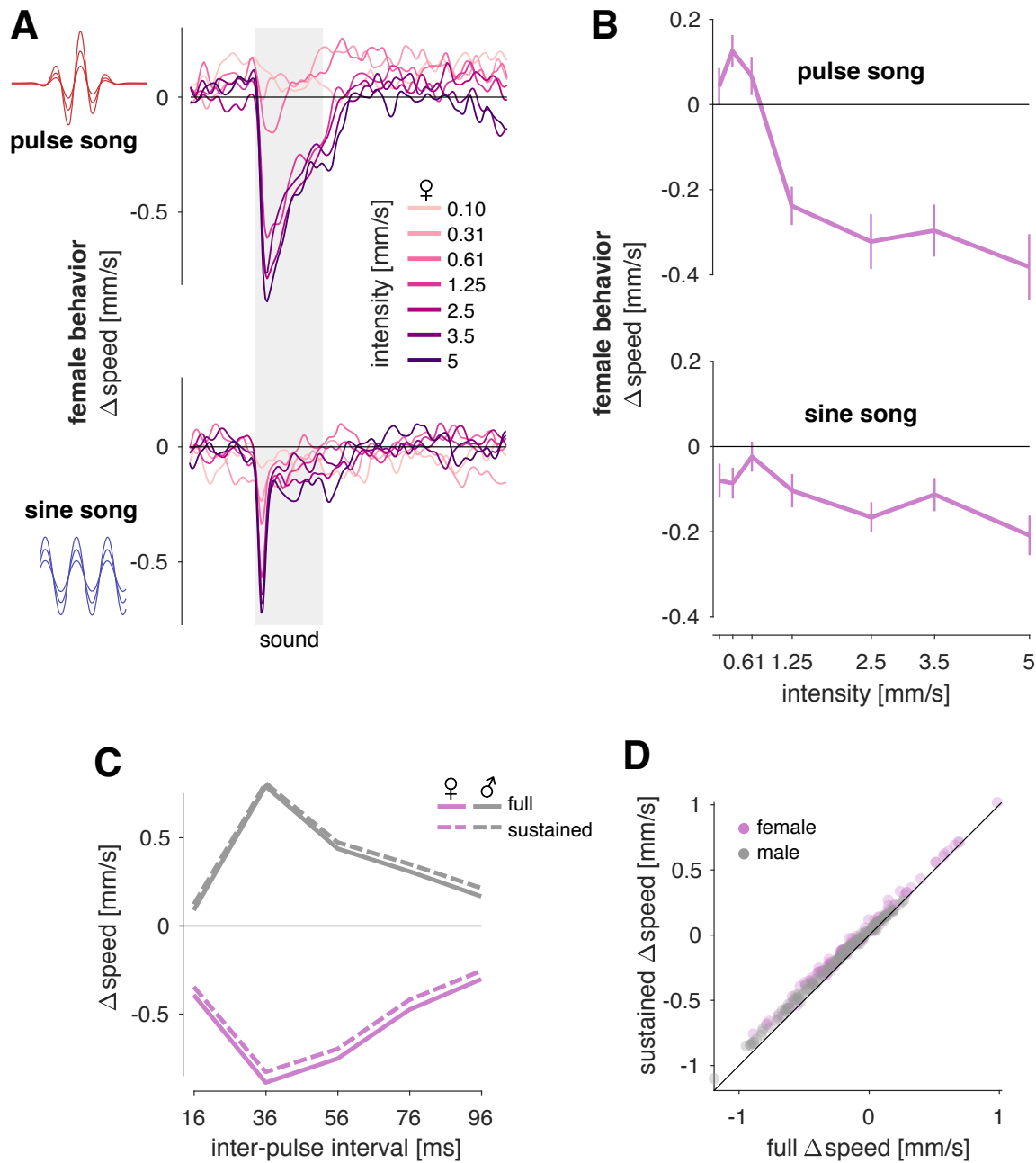


**Figure S1. Related to Figure 1.**

**A** Locomotor responses of females for pulse trains (36ms IPI stimulus) and sine tones (100Hz tones) of different intensities (color coded, see legend). Intensity is given in mm/s since flies are sensitive to the particle velocity of sound, not sound pressure.

**B** Speed tuning curves for the traces in A obtained by averaging the speed in the six seconds following stimulus onset. For pulse song, responses are weak for intensities <1mm/s and don't change much beyond that. While sine responses are weak, there is a tendency for speed to change more for louder sine tones. Lines and error bars indicate mean $\pm$ s.e.m. over ~120 flies.

**C** Excluding the transient response component only negligibly affects behavioral tuning curves. Shown are IPI tuning curves for males (gray) and females (magenta) obtained by averaging different epochs of the speed traces. The full response (solid lines) corresponds to the average, base-line subtracted speed in the 6 seconds following sound onset. For the sustained response (dashed lines), we start integration of the speed traces not at sound onset but 500ms into the sound. Tuning curves for the full and sustained phases are very similar – the negative transient response component adds only a weak negative bias to the tuning curves.

**D** Full vs. sustained responses for all stimuli tested in males (gray) and females (magenta). Both measures yield highly correlated responses ( $r^2=1.00$ ,  $p=2\times 10^{-284}$ ). The purely negative transient response component in the full responses adds a negligible negative bias of -0.05mm/s.

**Figure S2**

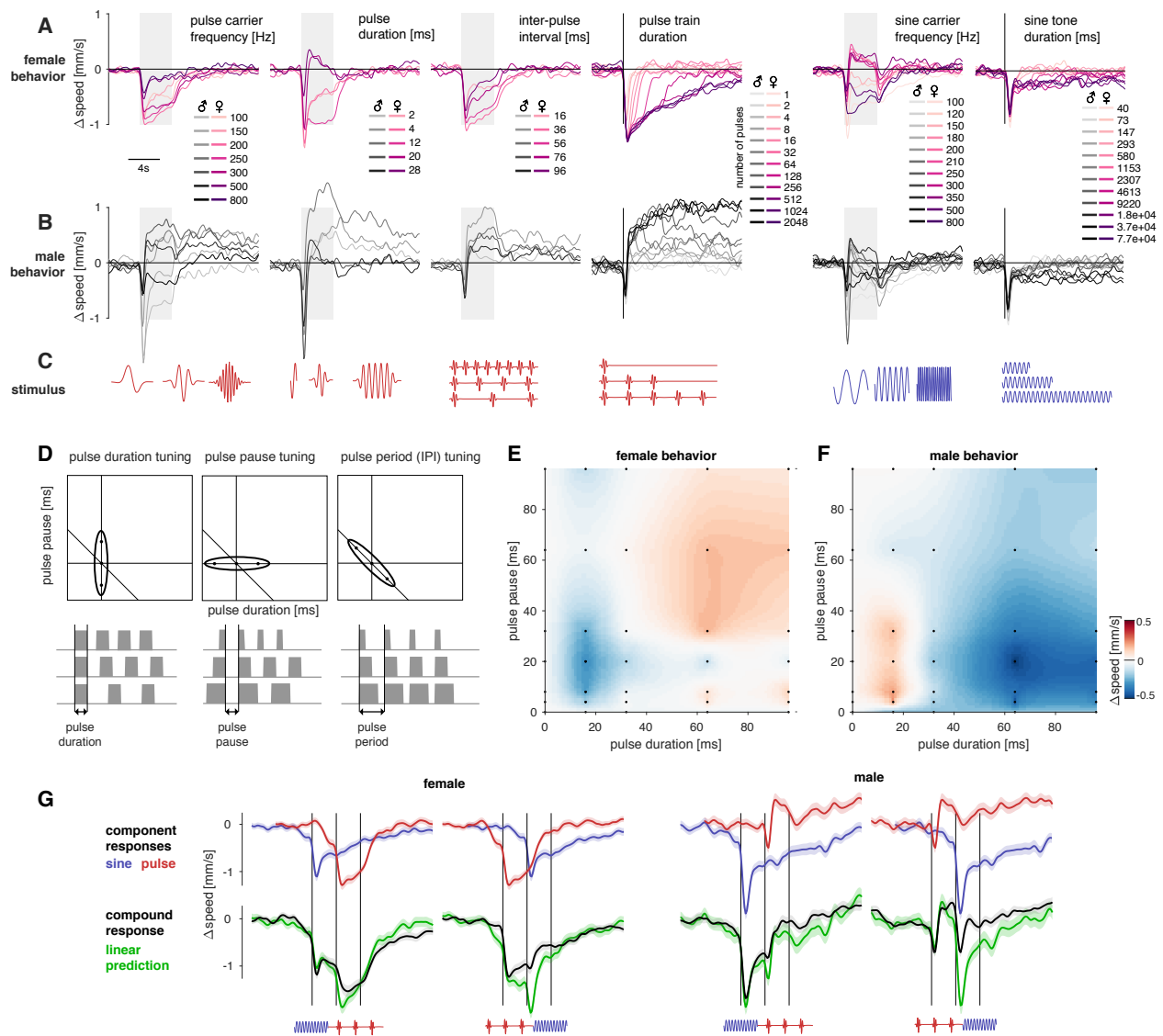


**Figure S2. Related to Figure 2.**

**A, B** Locomotor response traces for all stimuli in Fig. 2A, B for females (A) and males (B). Stimulus values are color coded (see legends). Gray shaded areas mark the duration of the sound stimulus. Vertical black lines indicate sound onset for stimulus sets with varying durations (pulse train duration, sine tone duration). Lines correspond to the mean over typically ~120 animals (see supp. table 1 for exact values). Error bars are similar to those in 1C and omitted for clarity.

**C** Pictograms (not to scale) illustrating each song feature examined in A-B. Pulse and sine song features are marked red and blue, respectively.

**D** Three principal types of tuning are observable when testing behavioral responses for stimuli with different pulse durations and pauses. Black ellipses indicate the range of stimulus parameters that evoke strong behavioral responses, dots correspond to the three (gray) stimuli shown below each tuning field. Horizontal, vertical, and anti-diagonal lines mark stimuli with constant pause, duration and period, respectively. Pulse duration tuning (left) corresponds to high selectivity (narrow tuning) for pulse duration and higher tolerance for pulse pauses. Pause duration tuning (middle), corresponds to high selectivity for pulse pause and high tolerance for pulse pause. Note that for both types, the tuning for pulse duration and pulse pause does not interact – e.g. the preferred pause does not change with pulse duration. Pulse period (a.k.a. inter-pulse interval) tuning (right) corresponds to a preference for stimuli with a constant pulse period, given by the sum of pulse duration and pause. For this type of tuning, pulse duration and pulse pause interact – the preferred pulse pause increases with decreasing pulse duration.

**E, F** Locomotor responses of females (E) and males (F) for pulse trains with different pulse durations and pulse pauses. Speed values are color coded (see color bar in F). Black dots mark the parameter combinations of the stimuli tested in FLyTRAP. Intermediate values were obtained using interpolation (see methods). Male and female response fields are similar except for the sign – females tend to slow (blue colors), males tend to accelerate (red colors), and vice versa (compare Fig. 2C). Responses are more selective for pulse duration than for pulse pause and pulse duration tuning is relatively independent of the pulse duration.

**G** Responses to sequences of sine tones (blue) and pulse trains (red). First and third row correspond to 2s sine followed by 2s pulse for females and males, respectively. For the second and fourth the order is reversed – stimuli start with 2s pulse song and transition into 2s sine song. The top row shows responses to the individual components of the sequence aligned to the onset of the component in the combined stimulus. The bottom row shows responses for both sexes to the compound stimuli (black) and the linear prediction obtained by summing the responses to the individual components (green). The linear prediction matches the measured responses well except at the transition due to transient response to sound onset only present in individual component responses. Lines and shaded areas correspond to the mean ± s.e.m. over 189 female and 217 male flies.

**Figure S3**

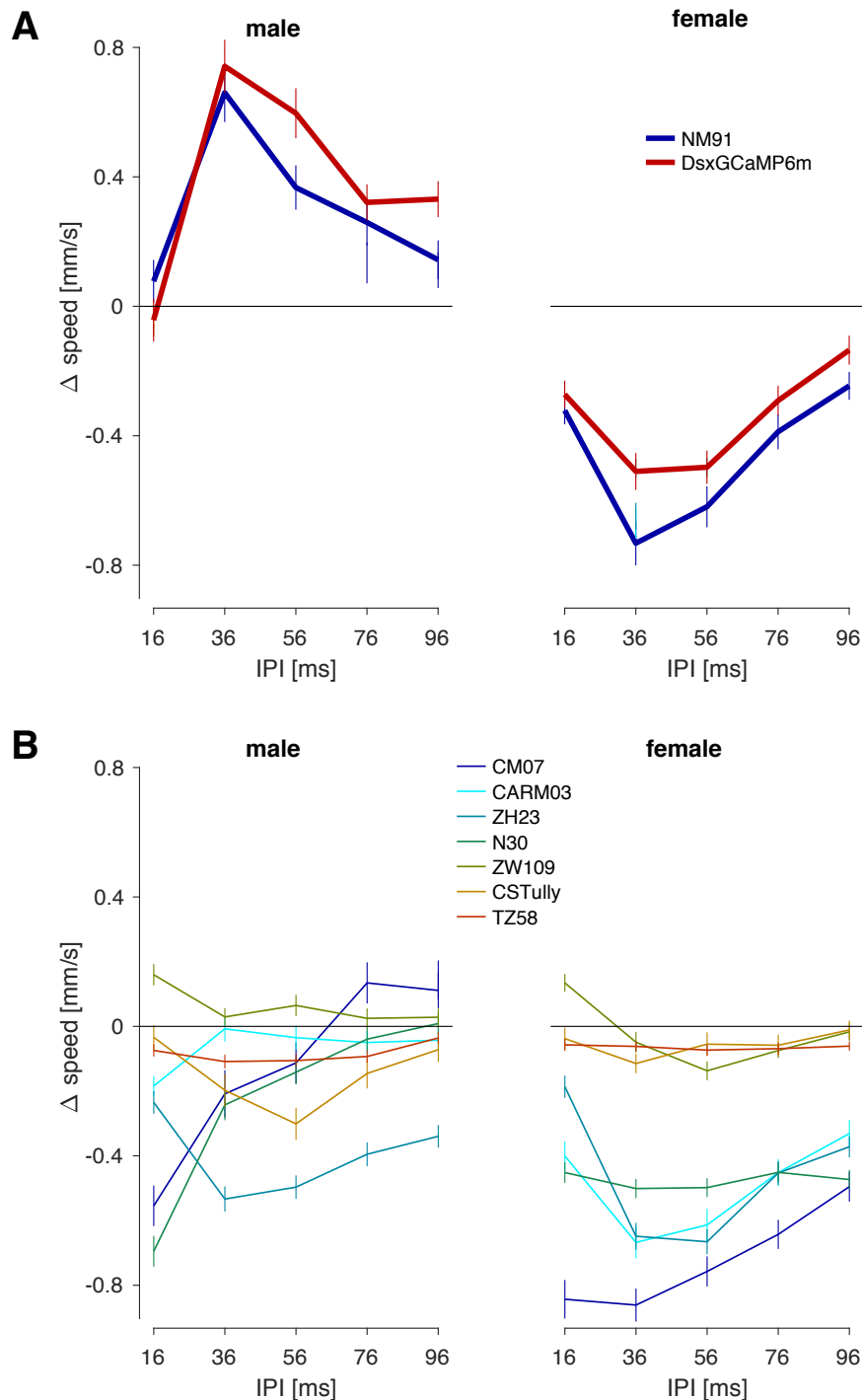


**Figure S3. Related to Figure 3.**

**A** Male (left) and female (right) locomotor tuning for pulse trains with different IPIs for NM91 – the wild type strain used in FLyTRAP – and flies expressing GCaMP6m in all Dsx+ neurons used for calcium imaging (see legend). Dsx-GCaMP6m and NM91 flies exhibit similar and species-typical IPI tuning that also matches the tuning found using alternative assays (see text for details).

**B** IPI tuning in seven additional wild type strains is diverse and not consistent with the species-typical tuning (male left, female right, see legend for strains used). Note, however, that most strains still respond sex-specifically to pulse song sex, similar to NM91 and Dsx-GCaMP6m. These strains produce similar responses to song in a natural courtship assay, suggesting that these strains require sensory cues that are missing in FLyTRAP for expressing their song preference.

Graphs show mean  $\pm$  s.e.m. over individuals (100-150 flies per strain and sex).

**Figure S4**

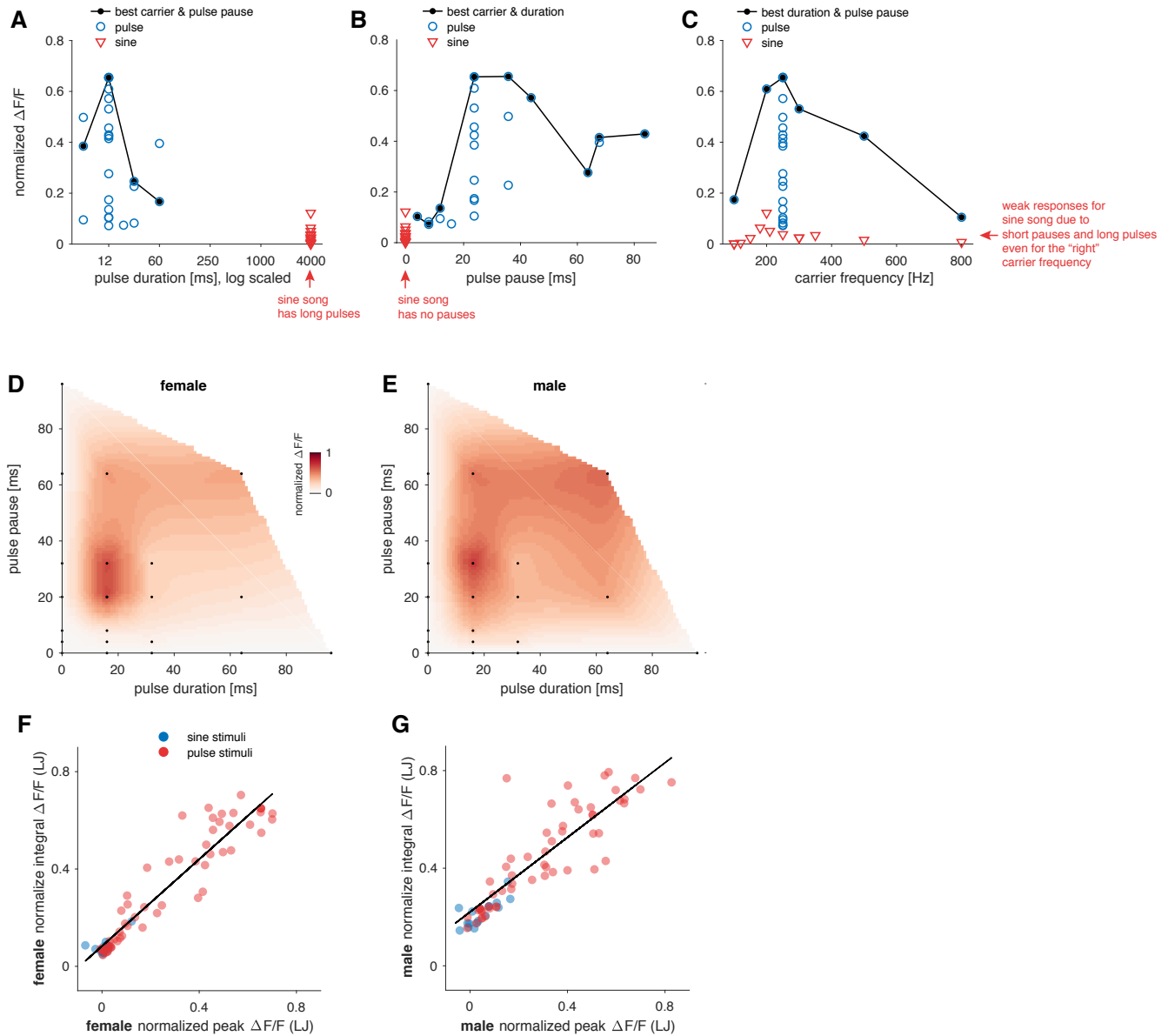


**Figure S4. Related to Figure 3.**

**A** Calcium response of the female LJ as a function of the pulse duration for all stimuli in our data set with a duration of 4 seconds. Blue circles correspond to pulse stimuli and red triangles mark sine stimuli, which by definition do not have pauses and can be thought of as very long pulses. Note that besides pulse duration, all stimuli also differ in pulse pause duration and carrier frequency – for instance all sine stimuli (red triangles) differ in carrier frequency (see C). This explains why stimuli with the same pulse duration evoke diverse calcium responses (integral  $\Delta F/F$ ) - they differ in these other stimulus features. The black line connects stimuli that have the optimal pulse carrier frequency (250 Hz) and pulse pause (20ms). To account for differences in  $\Delta F/F$  across individuals, values were normalized by the maximal  $\Delta F/F$  for each individual.

**B** Same calcium response data as in A but now plotted as a function of pulse pause. Sine stimuli correspond to pulse trains with no pauses – they are by definition continuous oscillations. The black line connects stimuli with the optimal pulse duration (12ms) and pulse carrier frequency (250Hz).

**C** Same calcium response data as in A but now plotted as a function of pulse carrier frequency. Sine stimuli differed in their carrier frequencies. The black line connects stimuli with the optimal pulse duration (12ms) and pulse pause duration (24 ms).

**D, E** Calcium responses from the female (D) or male (E) LJ for pulse trains with different combinations of pulse pauses and pulse durations. The stimuli constitute a subset of those measured in the behavior. LJ tuning for pulse trains with different pulse pauses and pulse durations recapitulates the behavioral tuning (compare Fig. S2E, F): LJ responses are more selective for pulse duration and the preferred pulse duration does not change with pause duration.

**F, G** Comparison of peak and integral  $\Delta F/F$  values from the LJ for all stimuli tested in females (F) and males (G). Pulse and sine song are marked with red and blue, respectively. The black lines correspond to the best linear fit. Both measures of calcium responses are highly correlated (males:  $r=0.79$ ,  $p=4\times 10^{-26}$ , female:  $r=0.80$ ,  $p=5\times 10^{-39}$ ).

**Figure S5**

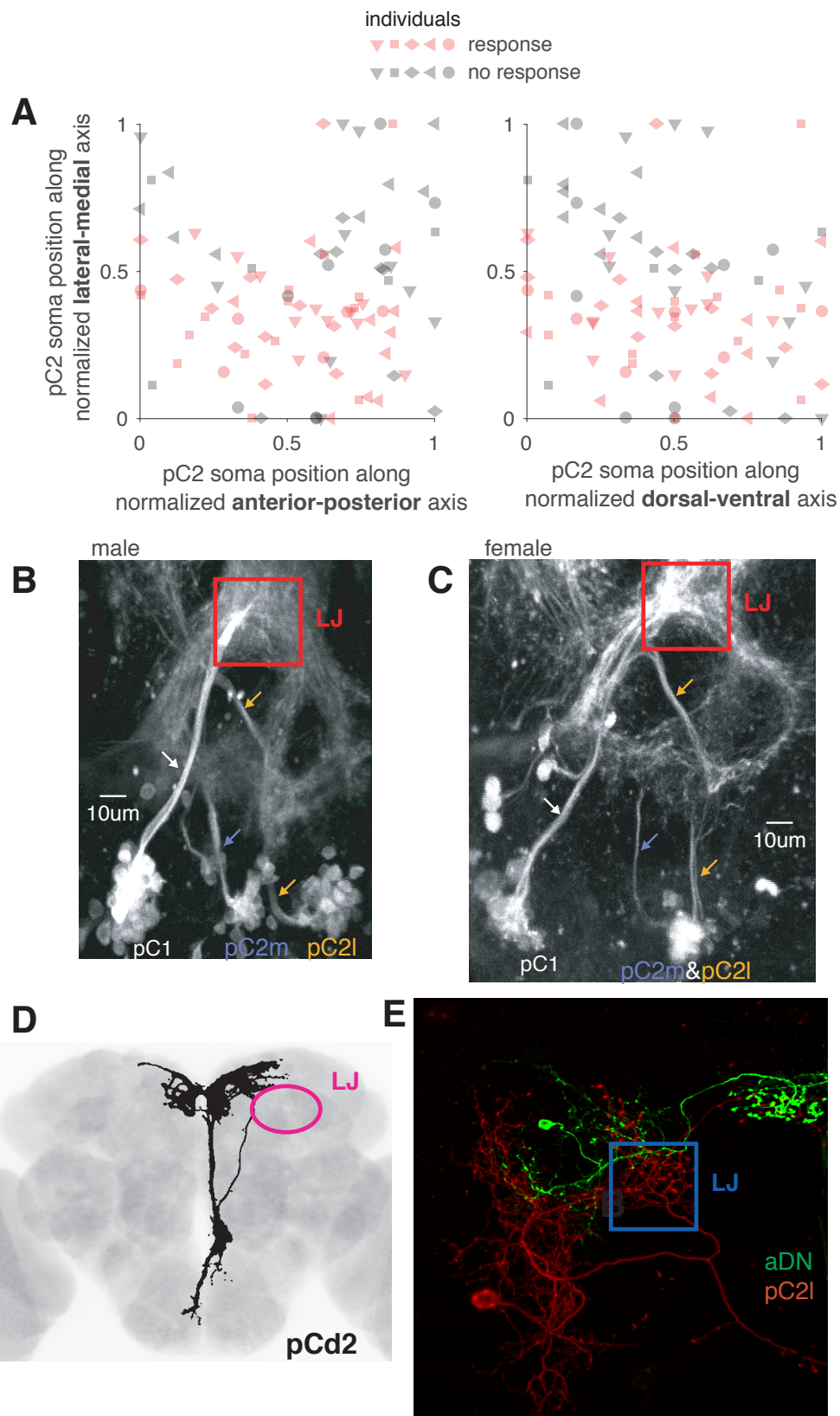


**Figure S5. Related to Figure 4.**

**A** Locations of pC2 somata in the female brain with (pink) or without (grey) auditory responses along the lateral-medial and anterior-posterior (left) or dorsal-ventral (right) axis. Soma positions were normalized to between 0 and 1 for each animal. Individual symbols (see legends) correspond to somata from different animals. Responsive pC2 somata are concentrated in the lateral proportion of the cell cluster (lower half of each plot) and largely correspond to the pC2I subcluster, although we also observed auditory responses in pC2m somata (see Movie S5).

**B, C** Max z-projection of baseline fluorescence values from a two-photon volumetric scan of a male (B) and female (C) brain expressing GCaMP6m in all Dsx+ neurons. Each of the three clusters (pC1 - white, pC2m – blue, pC2I - yellow) connects to the LJ (red) via unique processes (arrows). pC2I and pC2m are hard to distinguish by soma location in many flies (mostly females) since they are intermingled.

**D** A single pCd2 neuron labeled using MCFO (black) registered to a template brain (JFRC2, gray). The lateral junction (LJ) is marked in magenta. pCd1 (not shown, {Kimura:2015ff}) and pCd2 do not project to the LJ.

**E** Max z-projection of a confocal stack in which aDN (green) and pC2I (red) were labelled with different colors using MCFO. pC2I but not aDN projects to the LJ (blue).

**Figure S6**

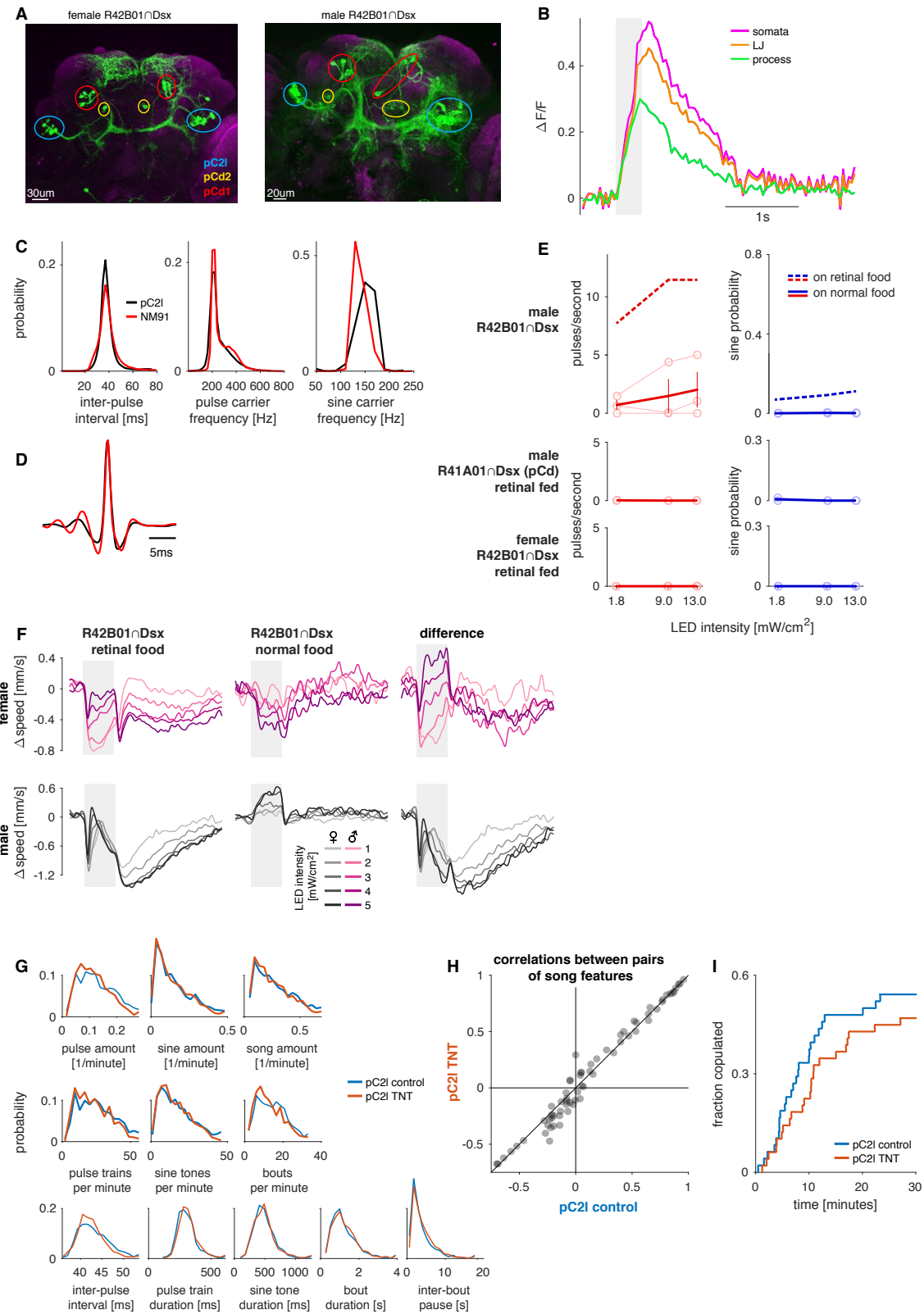


**Figure S6. Related to Figure 5.**

**A** Expression pattern of CsChrimson.mVenus in the intersection of R42B01 and Dsx (green) for females (left) and males (right). Neuropil is labelled with nc82 (magenta). The intersection labels 11/22 female and 22/36 male pC2I neurons, as well as 5-6 pCd1 and 2 pCd2 in either sex

**B** Calcium responses from a female of this line for pulse trains (IPI 36ms) in pC2I somata (blue), the pC2I process (yellow) and the LJ (red). We detected auditory response in all 5 pC2I cells visible in the imaging plane, as well as in the LJ and in the pC2I process.

**C, D** Song evoked by 655nm activation of R42B01 $\cap$ Dsx neurons (black, N=7 flies) resembles the natural song produced by wild type flies (NM91, N=47 flies) during courtship (red). Shown are distributions of IPIs, pulse carrier frequencies, and sine carrier frequencies (C) as well as average pulse shapes (D).

**E** Pulse rates and sine song probability upon optogenetic activation of males expressing CsChrimson (red-shifted channel rhodopsin) in R42B01 $\cap$ Dsx (see A) on food without added retinal (top, solid lines, N=3 flies) or on food with retinal (top, dashed lines, N=7 flies), males expressing CsChrimson in R41A01 $\cap$ Dsx (labels pCd1) fed retinal food (middle, N=2 flies), and females expressing CsChrimson in R42B01 $\cap$ Dsx neurons fed retinal food (bottom, N=3 flies). Optogenetic activation of pCd1 in the male (middle) and of pC2 (and pCd) in the female (bottom) does not evoke song, demonstrating that the singing evoked by R42B01 $\cap$ Dsx activation in males is 1) due to pC2 and not the pCd1 also labeled in this line, and 2) sex-specific. Males expressing CsChrimson in R42B01 $\cap$ Dsx that were kept on normal food produced some song upon activation, though much less than males fed retinal (see dashed lines). This residual activation likely stems from small amounts of retinal in normal food.

**F** Speed traces for female (magenta, top) and male (grey, bottom) flies expressing CsChrimson in R42B01 $\cap$ Dsx. Shown are responses for flies fed retinal (left), normal food (middle) and the difference between the traces of retinal and normally fed flies (right). Colors correspond to different driving voltages of an array of 655nm LEDs. Lines correspond to averages over 70 females and 83 males fed retinal food, and 29 female and 34 males fed normal food.

**G** Statistics of male song do not change when they court pC2I TNT females (using the R42B01 $\cap$ Dsx driver). Shown are distributions of 11 song parameters from NM91 males courting pC2 control (blue) or pC2 TNT females (orange).

**H** Female genotype does not change correlation statistics (correlations between pairs of song parameters) in the song of NM91 males. Shown are all unique pair-wise correlations between the 11 song parameters in F for the song of NM91 males courting pC2I control (x values) or pC2I TNT females (y values).

**I** Cumulative fraction of copulated pairs of NM91 males courting pC2I control (blue) or pC2I TNT females (orange). There is weak but statistically not significant effect of female genotype on copulation rates ( $p=0.19$ , Cox's proportional hazards regression model).

F-H: Data from 48 pC2 control and 48 pC2 TNT pairs.

**Figure S7**

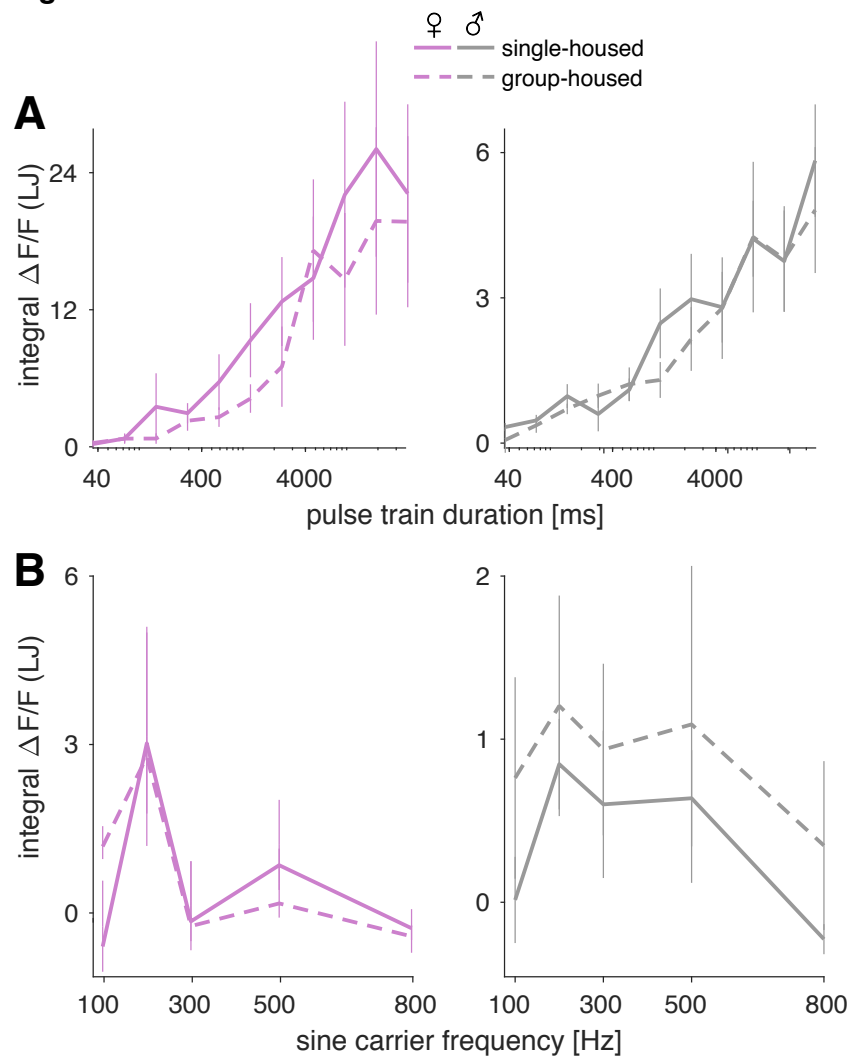


**Figure S7. Related to Figure 6.**

**A** Calcium responses in pC2 neurons (measured via the LJ) for pulse trains with different durations (IPI=36ms) in single- and group-housed (solid and dashed lines) females (left) and males (right). Data from 5-6 flies for each condition (single/group-housed, females/males).

**B** Same as A, but for sine carrier frequency. Data from 20/5 single/group-housed females and 12/6 single/group-housed males.

Responses to pulse trains with different durations and to sine tones with different carrier frequencies do not change substantially with housing conditions.

Lines and error bars correspond to mean  $\pm$  s.e.m over flies.

## Movie legends

**Movie S1** – Female flies (wild type NM91) in FLyTRAP. Track histories are shown as colored trails. Movie speed corresponds to real time.

**Movie S2** – Males extend their wings in response to pulse song in FLyTRAP. In this example, 10 out of 12 flies extended their wings after stimulus onset (4 second pulse train, inter-pulse interval = 36ms). Responding flies are marked with red circles. Movie is slowed down 4X. Some flies extend their wings spontaneously (not triggered by sound), see for example fly 5 in this movie.

**Movie S3** – Two-photon Calcium imaging of the female lateral junction and pC2I process. GCaMP6m is expressed in all the Dsx<sup>+</sup> neurons. The response in the lateral junction (LJ) and pC2I process are highly correlated (see also Fig 4F). Three responses are shown for a single fly – 4 second pulse trains with inter-pulse intervals of 16/36/76ms. The text in the corner appears when the sound stimulus is on. Movie speed corresponds to real time.

**Movie S4** - Two-photon Calcium imaging of the male lateral junction and pC2I process (same as in S3).

**Movie S5** – Two-photon Calcium imaging (single plane) of female pC2 cell bodies. The responses to a 4 second pulse train and to a 4 second sine tone (carrier frequency – 200Hz) are shown. In most females the pC2I and pC2m cell bodies can not easily be separated into distinct clusters. Movie speed corresponds to real time.

**Movie S6** – Two-photon Calcium imaging (single plane) of male pC2 cell bodies (same stimuli as in movie S5). pC2I and pC2m cell bodies can be spatially organized in two distinct clusters. Movie speed corresponds to real time.

**Movie S7** – Optogenetic activation of pC2I neurons in an isolated male. Three light intensities are shown (1.8, 9, 13 mW/cm<sup>2</sup>). Sound is recorded using microphones that tile the chamber floor. Video and audio are synced and played at real time.